2021-06

Autonomous Assessment of Satellite Ground Station Health

Wistner, Stephen A., II

Monterey, California. Naval Postgraduate School

NAVAL POSTGRADUATE SCHOOL

MONTEREY, CALIFORNIA

THESIS

AUTONOMOUS ASSESSMENT OF SATELLITE GROUND STATION HEALTH

by

Stephen A. Wistner II

June 2021

Thesis Advisor:	Giovanni Minelli
Co-Advisor:	Noah Weitz
Second Reader:	James H. Newman

THIS PAGE INTENTIONALLY LEFT BLANK

REPORT DOCUMENTATION PAGE			*Form Approved OMB No. 0704-0188*

1. AGENCY USE ONLY *(Leave blank)*	**2. REPORT DATE** June 2021	**3. REPORT TYPE AND DATES COVERED** Master's thesis

4. TITLE AND SUBTITLE AUTONOMOUS ASSESSMENT OF SATELLITE GROUND STATION HEALTH	**5. FUNDING NUMBERS**
6. AUTHOR(S) Stephen A. Wistner II	
7. PERFORMING ORGANIZATION NAME(S) AND ADDRESS(ES) Naval Postgraduate School Monterey, CA 93943-5000	**8. PERFORMING ORGANIZATION REPORT NUMBER**
9. SPONSORING / MONITORING AGENCY NAME(S) AND ADDRESS(ES) N/A	**10. SPONSORING / MONITORING AGENCY REPORT NUMBER**

11. SUPPLEMENTARY NOTES The views expressed in this thesis are those of the author and do not reflect the official policy or position of the Department of Defense or the U.S. Government.

12a. DISTRIBUTION / AVAILABILITY STATEMENT Approved for public release. Distribution is unlimited.	**12b. DISTRIBUTION CODE** A

13. ABSTRACT (maximum 200 words)

The objective of the study was to develop the initial capabilities enabling the eventual automation of an antenna gain-to-noise-temperature (G/T) measurement process using a software defined radio. This research investigated how to improve the Mobile Cubesat Command and Control (MC3) network's ability to remotely monitor a ground station's health. Previous thesis work was leveraged to collect baseline data and process it using software created by the Space Dynamics Laboratory for the MC3 program. The thesis required hands-on use of the NPS MC3 ground station and other stations on the network. The results of this thesis demonstrate that a software defined radio is capable of collecting and processing radio frequency signals from the sun and cold sky to produce a G/T value with enough fidelity to assess the health of the station's downlink radio frequency chain. Continued expansion of the collected frequency range by the software defined radio is recommended to provide a broader assessment of the antenna's sensitivity to weak, space-borne signals.

14. SUBJECT TERMS ground station, autonomous, G/T, USRP, SDR, Titan, radio frequency, sun, cold sky, moon, antenna	**15. NUMBER OF PAGES** 79
	16. PRICE CODE

17. SECURITY CLASSIFICATION OF REPORT Unclassified	**18. SECURITY CLASSIFICATION OF THIS PAGE** Unclassified	**19. SECURITY CLASSIFICATION OF ABSTRACT** Unclassified	**20. LIMITATION OF ABSTRACT** UU

NSN 7540-01-280-5500

Standard Form 298 (Rev. 2-89)
Prescribed by ANSI Std. 239-18

THIS PAGE INTENTIONALLY LEFT BLANK

Approved for public release. Distribution is unlimited.

AUTONOMOUS ASSESSMENT OF SATELLITE GROUND STATION HEALTH

Stephen A. Wistner
Lieutenant, United States Navy
BS, United States Naval Academy, 2015

Submitted in partial fulfillment of the
requirements for the degree of

MASTER OF SCIENCE IN SPACE SYSTEMS OPERATIONS

from the

NAVAL POSTGRADUATE SCHOOL
June 2021

Approved by: Giovanni Minelli
Advisor

Noah Weitz
Co-Advisor

James H. Newman
Second Reader

James H. Newman
Chair, Space Systems Academic Group

THIS PAGE INTENTIONALLY LEFT BLANK

ABSTRACT

The objective of the study was to develop the initial capabilities enabling the eventual automation of an antenna gain-to-noise-temperature (G/T) measurement process using a software defined radio. This research investigated how to improve the Mobile Cubesat Command and Control (MC3) network's ability to remotely monitor a ground station's health. Previous thesis work was leveraged to collect baseline data and process it using software created by the Space Dynamics Laboratory for the MC3 program. The thesis required hands-on use of the NPS MC3 ground station and other stations on the network. The results of this thesis demonstrate that a software defined radio is capable of collecting and processing radio frequency signals from the sun and cold sky to produce a G/T value with enough fidelity to assess the health of the station's downlink radio frequency chain. Continued expansion of the collected frequency range by the software defined radio is recommended to provide a broader assessment of the antenna's sensitivity to weak, space-borne signals.

THIS PAGE INTENTIONALLY LEFT BLANK

TABLE OF CONTENTS

LIST OF FIGURES

LIST OF ACRONYMS AND ABBREVIATIONS

AFIT	Air Force Institute of Technology
COTS	Commercial off-the-shelf
DOD	Department of Defense
EIRP	Effective isotropic radiated power
ERP	Effective radiated power
G/T	Antenna gain to noise temperature
GOTS	Government off-the-shelf
LEO	Low earth orbit
LNA	Low noise amplifier
MC3	Mobile CubeSat Command and Control
MEO	Middle earth orbit
NOAA	National Oceanic and Atmospheric Administration
NPS	Naval Postgraduate School
RF	Radio frequency
SDL	Space Dynamics Laboratory
SDR	Software defined radio
SNR	Signal to noise ratio
TT&C	Tracking telemetry and control
UAF	University of Alaska Fairbanks
UHF	Ultra high frequency
USRP	Universal software radio peripheral

THIS PAGE INTENTIONALLY LEFT BLANK

ACKNOWLEDGMENTS

My experience working on this thesis at NPS has been phenomenal, and all credit belongs with my advisor and co-advisor, Dr. Giovanni Minelli and Mr. Noah Weitz. To start, they were extremely welcoming and eased each of my concerns about attempting a thesis that was in an area in which I had very little experience, software and coding. They were very encouraging and reassured me that as long as I put the time in, my lack of experience would not be an issue. Not only did they encourage me with words, but they backed it up with their actions; I remain grateful.

Mr. Noah Weitz spent countless hours sitting next to me on the computer teaching me the language of coding. When adversity struck that forced us to work away from the lab, he also spent time helping me remotely. Let me be very clear, teaching me how to code was a very tall task and without question, underutilized his expertise; I did not take that for granted.

Dr. Giovanni Minelli constantly impressed me with how well he was able to successfully juggle all of his responsibilities working at NPS, managing the MC3 network, and advising multiple students on their theses. In spite of these vast challenges, somehow he made it feel like I was his highest priority and a member of the team. He allowed me to listen in on every aspect of his work while I was in the lab, which was a unique and rewarding experience. He taught me a great deal not only about the work related to my thesis, but also how to maintain a positive perspective in spite of the circumstances being faced.

I am extremely grateful to both Dr. Minelli and Mr. Weitz for all of their time and help with my thesis. There is no way I could have completed this thesis, or learned as much as I have without them. The time spent working with them, and the progress made with the MC3 network as a whole, have been amazing experiences that I will remember fondly.

THIS PAGE INTENTIONALLY LEFT BLANK

I. INTRODUCTION

A. THE WORLD STAGE

The increasingly proliferated use of the space domain by nations around the world continues to showcase the importance governments and companies place on operating spacecraft to further their needs. Starting with the space race of the 1960s, the United States has been actively operating in this domain, including placing the first man on the moon in 1969 for strategic and scientific merit. Since then, the world's space-based capabilities have expanded exponentially with no signs of abating. Though space has traditionally been the province of governments and militaries, as seen during the decades-long high-stakes standoff between the United States and the Soviet Union, the industry has recently shifted to lowering the barrier sufficiently such that private companies can also operate in the space domain for profit. Space also represents a symbolic opportunity to unify humanity despite political rivalries as seen by the creation of the International Space Station with the United States, Russia (the former Soviet Union), and others as key partners shortly after the aforementioned Cold War ended.

Moreover, the earth-sensing capabilities of overhead assets have dramatically improved in recent years. Governments and militaries have come to rely on these data products for intelligence gathering, weather prediction, and tracking large scale activities like shipping and transportation around the world. Companies are flying constellations of satellites to provide internet connectivity throughout the world, and there are unlimited possibilities that have yet to be conceived. The myriad nations' adventures into space have been dramatic, and have had an impact in seen and unforeseen ways. The impacts derived from space capabilities are only increasing as scientific breakthroughs are discovered and technological advancements are made. The U.S. space program has developed products and systems that have improved the quality of life for every American. The worldwide development of space capabilities has even begun to shift the global balance of power. The countless discoveries derived from space exploration are increasing as rapidly as scientific breakthroughs and technological advancements can allow. The U.S. has recognized the importance of space, not only with regard to science and technology, but also to national

security. The formation of the United States Space Force at the end of 2019 demonstrates that priority. As space capabilities progress so will their impact on shaping how we interact with the world.

One of the biggest ways that space is currently leveraged is through the transfer of information and data. Data move through space in a variety of paths, speeds, and quantities. Data can be sent from a ground station somewhere on Earth to another ground station on the other side of the planet via a satellite in space. Data can also be transferred from one satellite to a ground station and vice versa. Each path in which that data travels can vary in both the amount of data and the rate, or speed of that data; both of those depend on the equipment used on the satellites or ground stations involved.

What makes transferring data across ground stations and satellites in space unique from other modern telecommunication methods is that continuous access is not guaranteed and relies on the geometry of the spacecraft's location with respect to the terrestrial station. While an email arrives almost instantaneously after it is sent, communication between a satellite and ground station can only occur during limited windows of time when they can "see" each other. When attempting a transmission of an electromagnetic message when either the satellite or ground station are not in sight of one another, the Earth occults the signal path and attenuates electromagnetic waves to unusable levels. The physics of using electromagnetic waves to transmit messages is what compels us to only communicate when a direct line of sight is achieved.

The limiting factor for a ground station to access a satellite is the altitude of that satellite. In general terms, the altitude of the satellite dictates its speed. The speed of the satellite determines the amount of time the satellite will be overhead and can be "seen" from the ground station. The speed of the satellite also dictates how long it will take for the satellite to return to the overhead position after it orbits out of sight of the ground station. A general example for reference is that a low earth orbit (LEO) satellite, with an altitude of 500 kilometers, can communicate with a ground station for only a matter of minutes, while it will take about 90 minutes for the satellite to orbit the Earth. A geosynchronous satellite, such as one of the National Oceanic and Atmospheric Administration's imagery satellies, are always in view of the Earth, however, require a substantially greater altitude

and continuous position maintenance to mitigate drift. Another matter compounding the difficulty of maintaining the line of sight that is required for communication, is that the Earth also rotates out of the satellite's orbital plane. When this occurs, there is potentially no contact between the satellite and ground station for several hours as a consequence. The aforementioned requirements for line of sight of communications, combined with the increasing demands for satellite communication, demonstrates the importance of ensuring the quality and reliability of those communication transmissions.

B. THE PROBLEM

Satellites are space vehicles that have a wide range of capabilities. Most generally, they are capable of collecting and transferring various forms of data, such as positional data used for navigation, remote sensing, weather, and pictures, to name a few. Satellites are capable of transferring or communicating data between other satellites or antennas on the Earth's surface; the terminals on Earth's surface that communicate with satellites are referred to as ground stations. These ground stations provide the infrastructure capable to monitor, collect, communicate, and service the satellites they manage. Satellites and ground stations all over the world are communicating and transferring data continuously and generally without issue. Without warning, however, a satellite will fail to communicate or transfer data with a ground station.

Let us postulate a hypothetical first failure that has occurred. For the operator of the ground station that is communicating with the satellite, this might rise to the level of immediate investigation. However, it is possible the response would be delayed for myriad reasons, such as workload and/or inattention. Additionally, without the right notifications, operators may miss anomalies altogether. It is conceivable that the problem persists as more failed passes occur and the ground station operators are unable to quickly determine the cause. Without the capability to monitor the health of the system there are limited ways to troubleshoot any anomaly, much less take proactive action to avoid failures.

In the event of an anomaly, there are two places to start troubleshooting efforts: on the spacecraft or the ground station. An immediate course of action might include: Were there any telemetry points on the spacecraft that suggest an impending issue? Is the

spacecraft working well with other stations? If no and yes respectively, then operators shift their attention to the ground station. Conducting troubleshooting efforts on a ground station can become complicated due to the often distributed geography involved, particularly if the affected ground station is on the other side of the country, or world, from the operators.

Under normal circumstances, traveling to a ground station would be a cost-intensive problem. Logistics also need to be coordinated to fly a team of technicians out to the location of the ground station. Once at the ground station, a thorough inspection would be required, which would take a minimum of a few days. Hardware, software, and the radio frequency (RF) health (the data transfer link) between the satellite and ground station would be inspected. Data collection and measurements would be taken over the course of a few days as well. The financial burden and the time needed to effectively troubleshoot a ground station is significant. A cost-benefit analysis would need to be conducted to determine if the prohibitive cost, including the expense of the required travel, as well as lost productivity while the team is out of their office conducting their investigation, is worth absorbing to investigate any of the failures that may occur.

An example of exacerbated logistical complications arising from ground station maintenance-related travel were the travel restrictions imposed by governments all over the world in response to the coronavirus (COVID-19) pandemic from 2020–2021. During the period of time this thesis was written, air travel to certain locations domestically and abroad was completely banned or three to fourteen day quarantines were required before and after travelers arrived at certain locations [1]. Even at most of the ground stations, access was limited to an arbitrary number of people determined by the local government or governing institution, further adding complexity to this situation. While the COVID specific restrictions are most likely "temporary," if the restrictions imposed all over the world in response to COVID is the new precedent for the handling of all future viruses of this magnitude, it would be prudent to have a plan in place to deal with the added challenges those restrictions pose. Sending a team of technicians to troubleshoot a ground station domestically or internationally was already a challenging task that dramatically increased in difficulty with the various travel restrictions. The complexity of the COVID restrictions

created many new hurdles and made it extremely difficult to execute the many facets of continuous spacecraft operations as well as the full scope of this research.

Space capabilities are growing and the ability to monitor and maintain the health of a ground station is difficult under normal circumstances. Combine that with the restrictive climate as inherent in a response to a virus, as well as any unforeseen future challenges, it is imperative to find a solution that can assist in troubleshooting any satellite to ground station issues. This leads to the questions worth researching.

C. RESEARCH QUESTIONS

How can the ability to monitor a satellite ground station's health and performance be improved?

A method to monitor the health of an MC3 ground station does currently exist. One method involves determining the antenna gain to noise temperature, or G/T of a ground station. G/T is a metric that helps characterize the antenna's performance regarding the system's sensitivity to weaker signals [2]. G is the antenna gain at the receive frequency measured in decibels and T is the noise temperature of the receiving system measured in Kelvin. The higher the ratio, the greater the ability of the antenna to detect a weak radio signal. G/T will be discussed in detail in the next chapter. However, it is important to understand that G/T is a metric that characterizes the antenna's performance, more specifically, regarding the system's sensitivity to weaker signals. Collecting the RF signal from the sun and comparing that signal to the one collected from the cold sky is a technique used to calculate the G/T of a system within 1 dB of accuracy [3]. Each ground station has a theoretical G/T based upon the various specifications of the equipment used, such as the size of antenna, length of cables, and quality of the feedhorn to name a few [4]. The higher the G/T value is overall, the better that system will perform. More importantly, the closer the practical G/T value is to the theoretical value the better a ground station is performing relative to its maximum capability.

The physical process of calculating the G/T value is relatively simple. However, without the appropriate tools to perform remote measurements, it requires sending a team of technicians to the location of the ground station to perform measurements over the

course of a few days. The collection process takes multiple days in order to ensure a substantial sample size is collected to provide useful feedback to appropriately address the potential issues. The extensive resources required to perform this health check naturally deter ground station operators from proactively taking these measurements. There is little desire to prioritize the resources required for an issue that does not yet exist. Therefore, this health check is mostly used as a troubleshooting method after a failure has occurred. The desire for feedback prior to a failure leads to the next question.

How can a ground station automatically conduct a daily health assessment that provides specific and actionable feedback to the user regarding any issues with the system?

If a ground station were capable of conducting this health check automatically, this would solve the manpower logistical hurdles, saving time and money, while providing a much larger sample size of values to analyze. Thanks to Bastian Beicher, a German military graduate student from the Bundeswehr University Munich, who conducted research at the Naval Postgraduate School (NPS), his thesis and previous work created software that would enable the G/T measurement to be taken with minimal operator intervention, utilizing a FieldFox spectrum analyzer [5]. A FieldFox spectrum analyzer is used primarily to measure the power of various frequency spectrums. Although the process for calculating G/T that resulted from his work required some operator input, it was heavily automated, and a necessary step to prove that it is possible to perform this health check with enough fidelity to provide useful feedback.

Unfortunately, a FieldFox spectrum analyzer can cost more than $80,000, and few ground stations are equipped with one. Utilizing the FieldFox for this measurement is beneficial during ground station maintenance; however, procuring enough FieldFox units for continuous monitoring is not a scalable nor a long-term solution as it is cost prohibitive. For this new process to be viable, this measurement would need to be taken with equipment that every ground station possesses, or can procure with minimal investment. To address that issue, the next research question is as follows.

How can this process of measuring and calculating G/T with the FieldFox be replicated to enable a universal software radio peripheral (USRP) to take the same measurement?

A USRP is a software defined radio (SDR) that is used for various RF applications. USRPs are much cheaper, at around $3,000, and every MC3 ground station is equipped with one. This means a solution utilizing a USRP would meet the criteria for a scalable solution. Once the G/T process is made automatic, and conducted daily using a USRP, the following research question arises.

How can this process provide actionable feedback to improve the system's performance and reduce the number of failed passes?

The ability to calculate the G/T remotely and automatically would eliminate the need to fly a team to the ground site to conduct the measurements; however, that ability alone would not reduce the number of failed passes. The next logical step, once the G/T calculation is automatic and able to be conducted daily with a USRP, would be to maximize the benefit of the information to reduce failures in communication between satellites and ground stations. In order to take proactive steps to avoid lost data transfers, the ability to recognize shifts in performance is necessary. Therefore, measuring the G/T daily, and storing those values in a database would enable trend analysis by the operations team. For example, if the team noticed the value was slowly falling each day over the course of a one-week period, this would indicate a decrease in performance, which may correspond to an impending equipment failure. This would prompt an investigation into the potential issue proactively, before a complete failure occurs. However, this process of reviewing the G/T trends stored in a database still requires user intervention. The next step would be to figure out how to automate that process as well, leading us to the next research question.

How is an alert created to force a user to acknowledge any issues derived from the health check?

Taking the proactive concept a step further, if the system was able to alert operators when the measurement falls below a determined value, that would allow for a more automated experience. By creating an automated alert when the system falls outside the

desired specifications, an operator would not be required to routinely review the system's health. Instead, the system would prompt the operator when intervention was required. Reliable alerting frees the operator to review performance data as part of periodic preventative maintenance as opposed to an actively monitored activity.

D. HYPOTHESIS

It is clear that the ability to automatically monitor the health of a satellite ground system is becoming more important as the capabilities of satellites improve at an increasing pace. Not only is it important to ensure maximum capability and functionality from the space assets, but it is also important to preserve and maximize scarce resources such as time and money. This is an extensive problem, and there are likely many different solutions and approaches that can provide a sufficient resolution.

The solution, or end result desired, is already known; the challenge is determining the most productive way to arrive at that destination and trust the results. We will attempt to mimic the results achieved from the FieldFox using a USRP, which should provide the capability to remotely monitor the health of a ground station. If the USRP can provide similar fidelity to an $80,000 spectrum analyzer, that would be a significant step toward creating a scalable solution to this problem. NPS's Mobile CubeSat Command and Control (MC3) program has access to the code created by Space Dynamics Laboratory (SDL) that analyzes RF signals using a USRP. This code was analyzed and configured to better integrate it with MC3 and the automated G/T application described in this thesis.

E. METHODOLOGY

For the purposes of this thesis and research, it was important to become familiar with the process of manually taking the G/T measurement to understand the intricacies involved, and help develop a solution that is easy for the operator to use. This understanding provided a solid foundation to build from when reviewing the code written for the FieldFox spectrum analyzer. Once familiar with the manual G/T process, we reviewed the code written for the FieldFox spectrum analyzer, and assessed the strengths and weaknesses. This helped determine what methods worked well, and which ones needed improving when trying to recreate that process for the USRP. After this step was

completed, we began investigating the SDL code utilizing the USRP. One of the objectives in this thesis was to determine if the SDL code would get us closer to automating the G/T calculation with a USRP, and if it was worth spending time investigating. One possible outcome was that the SDL code would have limited value, in which case it would have been a more efficient use of time developing code from scratch. Once it was determined that the SDL code was worth spending time investigating, the next step was to test and refine the code.

It was unclear if the USRP was capable of producing a G/T measurement with the fidelity required to meet the purposes of this thesis. Validating the code and USRP measurements to a point where the results could be trusted was the next step. Could the results be trusted, and did the results help get us closer to the end goal for this thesis? Once we were comfortable with the results, the next steps were to refine, automate, and improve the entire process as much as possible. Steps were taken by Ron Phelps, a software engineer for the NPS MC3 team, to create a database to store the results. Some of the last steps of this thesis involved an investigation into alerts that would notify the user of a potential issue determined by a G/T value outside of the desired specifications. Finally, a G/T calculation was conducted remotely at NPS involving three ground stations in the MC3 network, all over the United States to validate the process, with those calculations assessed for improvements.

F. IMPORTANCE

There are, and likely will always remain, ways to improve and refine the G/T process. The scope of this research is not to develop the perfect solution to this problem. Rather, the goal is to develop the initial capabilities that will enable the eventual complete automation of the G/T measurement process and corresponding evaluation. When the G/T process becomes a finished and polished product, it has the potential to be scaled and used by not only the MC3 network, but also by any ground station within the Department of Defense (DOD) that would want access to this capability. This functionality would provide a quantitative way to measure the health of any ground station, and give visibility to any trends indicating degradation of the system. This would lead to the reduction of failed

communications between satellite and ground stations by allowing the operator an opportunity to take proactive measures and repair any issues before the failure occurs. Ultimately, this capability will save countless labor hours and extensive resources; therefore, the objective of this thesis is to get as close as possible to automating the G/T calculation with a USRP that would provide sufficient context to observe the health of a ground station.

G. SCOPE

This thesis attempts to measure and calculate the G/T utilizing the sun as the RF source. The other RF sources such as the moon, stars, or other satellites were not investigated in this thesis and are left as future work. The NPS ground station was where everything was developed, tested locally, with a few remote tests conducted involving the Air Force Institute of Technology (AFIT) and Space Dynamics Laboratory (SDL) ground stations. The USRP used was the National Instruments USRP 2922 driven by the SDL Titan software package.

H. ROAD MAP

In this thesis, Chapter II discusses in detail what G/T is, why it is used, how to calculate it, and other background information to develop a complete understanding of the process. Chapter III provides a quick review of other work conducted utilizing the moon and stars as the RF source for the G/T calculation, followed by exploring in further detail the methodology, hurdles, and steps taken to get closer to developing this process. Chapter IV explores the results of this thesis, and Chapter V discusses the conclusion and recommendations to further develop this process.

II. BACKGROUND

The Mobile CubeSat Command and Control (MC3) program is a DOD-led initiative, managed by the Naval Postgraduate School (NPS), which operates a network of nine satellite ground stations around the United States to support research and development activities in small satellites for the U.S. government. While MC3 is led by the DOD, it also supports missions with universities across the United States, as well as foreign nations, to provide educational and scientific learning opportunities [6], [7]. MC3 communication stations provide the infrastructure and support for CubeSats, a miniature satellite designed for space research. A CubeSat is built to standard dimensions called Units, or "U," of 10 cm x 10 cm x 10 cm and normally weighs less than three pounds [6]. With a combination of commercial off-the-shelf (COTS) and government off-the-shelf (GOTS) hardware and software, covering the frequency ranges in the X-band, S-band, and UHF radio spectrum bands. This research utilizes the S-band with a 3-meter parabolic dish to collect the RF signal from the sun and cold sky and calculate a G/T. The S-band refers to the two to four gigahertz range of the electromagnetic spectrum, and a parabolic dish is the reflective material that projects or collects that electromagnetic energy.

Communication between a ground station and a satellite at orbital altitudes ranging from a few hundred to several thousand–kilometers, involves many complex systems. Those systems make up the satellite link. The two ends of that link are the ground station and the satellite. Broadly speaking, a link is formed when the satellite transmits an RF signal that is received and amplified, and then the embedded message is demodulated by the ground station or vice versa [8]. The satellite link is discussed in greater detail in the next chapter.

Issues within the satellite communications process can vary significantly in type and magnitude. Determining the origin of an anomaly can require many hours, consume extensive resources, and incur a significant opportunity cost for the capability of that satellite. Furthermore, if the issue is with the satellite, physically accessing and troubleshooting that end of the link is very difficult.

In an effort to alleviate the burden of correcting a deficiency within the satellite communication link after it makes the link inoperable, this thesis contributed to developing an automatic process that will prevent these failures altogether. To that end, this chapter discusses in more detail what G/T is and its significance, followed by the justification for using the sun as the source of RF.

A. HOW DOES G/T BENEFIT GROUND STATIONS?

G/T is a performance metric for the ground station's antenna. Calculating and utilizing the G/T as a metric for the antenna's performance is common practice in the RF engineering industry. Factors that impact the noise temperature, or T, include terrestrial, cosmic, and thermal noise, as well as noise from the ground station and equipment [2]. Thus, G/T is a useful metric to verify the condition of an antenna, and determine possible antenna-receiver degradation of ground stations. The G/T can also be utilized as a quality assurance test to determine if a satellite communication ground station meets the desired standards of performance [2].

In addition, if the G/T values are stored in a database, the operators of the ground station can use those stored G/T values as a historical record of ground station performance. This database can help identify if any repairs or improvements are necessary to enhance the performance of the ground station, or if any degradation has occurred. The G/T value database can also be useful for providing quantitative feedback to determine the effectiveness of any upgrades made to a ground station. If G/T measurements are taken and stored daily, then any repairs or improvements to the ground station can be measured immediately; the new G/T values calculated after repairs or improvements have been made, can be compared to the prior G/T values to assess any impact on performance. Any measured increase in performance can be compared with the cost for that upgrade or repair, and a cost-benefit analysis can be built for future use in managing ground stations.

Each ground station or antenna will by design have a baseline G/T. Therefore, the measurement of G/T using the sun (or other celestial object) can be performed nearly as accurately, and in most cases, more accurately than measuring G and T separately [2]. Calculating and storing this ratio daily allows the user to determine deviations from that

baseline, which is a leading indicator of a potential problem to investigate further. Ultimately, the ability to notice potential issues early allows for troubleshooting efforts to correct the problem before it might otherwise require a complete shutdown of the system.

B. HOW TO CALCULATE G/T

In order to accurately calculate G/T, there needs to be a source of RF emissions. Such as another antenna (with known configuration), the moon, a radio star (Cassiopeia), or the sun [2]. Equation 1 is used to calculate the G/T [2]:

$$\frac{G}{T} = 10\log_{10}\left[\frac{8\pi k(y-1)}{S_0\lambda^2 C\alpha}\right], \tag{1}$$

where

$\frac{G}{T}$ Calculated G/T of antenna system, dB/K

k Boltzmann Constant = 1.38 x $10^{-23} W/K/Hz$

y Delta of source noise power density to cold sky power density, linear no units

S_0 Solar Flux Density, expressed in solar flux units (SFU) $10^{-22} W/m^2Hz$ (if the sun is chosen as the source of RF emissions)

λ Wavelength in meters

C Beam Correction Factor, linear no units

α Atmospheric Attenuation at elevation angle, linear no units.

The following sections examine each of these variables in detail.

1. Received Power Delta (*y*)

The *y*-factor is the most important measurement to determine the G/T because the *y*-factor has the most significant impact of all the variables on the calculation [9]. Within

the solar G/T calculation, the *y*-factor, or *y,* signifies the difference in power received from the RF source (the sun) vs. the cold sky. To obtain this measurement, the ground station antenna points at the RF source to record a power level (P_{source}). Then the antenna points roughly 30 degrees away at the same elevation to record a power level of the cold sky ($P_{coldsky}$) [9]. It is not necessary for the antenna to be rotated exactly 30 degrees; it need only point far enough away from the sun that the radiated RF power does not significantly contribute to the cold sky RF collection.

The difference between P_{source} and $P_{coldsky}$ determines the P_{delta} which is converted from the decibel scale to obtain a linear value (y), shown in Equations 2 and 3 [9]:

$$P_{delta} = \left| P_{source} - P_{coldsky} \right| \text{ and} \tag{2}$$

$$y = 10^{\frac{P_{delta}}{10}}, \tag{3}$$

where

P_{delta} Difference between system noise power density when the antenna is looking at the RF source and cold sky in dB

P_{source} Power in dB received by the antenna system when pointed at the RF source

P_{coldsky} Power in dB received by the antenna system when pointed at cold sky, at the same elevation as P_{source}

y Linear representation of P_{delta}.

To ensure that the *y*-factor is accurate, a P_{delta} value of 1 dB or greater is necessary. With a P_{delta} value less than 1 dB, the G/T calculation can yield results that provide no practical value [9].

2. Solar Flux Density (S_0)

The solar flux density is the amount of solar energy per unit area [10]. Solar flux density can be calculated at the ground station; however, that calculation is computationally intensive. Instead, an industry standard already exists that provides a value with enough precision to calculate the G/T. The National Oceanic and Atmospheric Administration (NOAA) calculates the solar flux density at various frequencies ranging from 245 MHz to 15.4 GHz. NOAA calculates the solar flux density by measuring the strength of solar emissions over the course of an hour at various locations, using two small radio telescopes or flux monitors [10] and averaging them. In order to acquire a solar flux density at the desired frequency, interpolation of NOAA's values using Equation 4 is necessary [5]:

$$I_e = \frac{\log_{10} \frac{f_{GT}}{f_2}}{\log_{10} \frac{f_1}{f_2}}, \tag{4}$$

where

I_e Interpolation Exponent

f_{GT} G/T Measurement Frequency (Hz)

f_1 Lower Flux Measurement Frequency (Hz)

f_2 Higher Flux Measurement Frequency (Hz)

Once the interpolation exponent is calculated, the solar flux density is interpolated using the flux measurement at $f_1(f_{m1}), f_2(f_{m2})$, and the interpolation exponent I_e [9];

$$S_0 = f_{m2}\left(\frac{f_{m1}}{f_{m2}}\right)^{I_e}, \tag{5}$$

where

S_0 Solar Flux Density (Interpolated) in Solar Flux Units (10^{-22} W m^{-2} Hz^{-1})

f_{m2} Flux Measurement at the Higher Flux Frequency (f_2) (10^{-22} W m^{-2} Hz^{-1})

f_{m1} Flux Measurement at the Lower Flux Frequency (f_1) (10^{-22} W m^{-2} Hz^{-1})

I_e Interpolation Exponent

While interpolating the solar flux density from values provided by NOAA is not the most accurate method, it is the most commonly used. Factors that impact the reliability of this measurement include latitude and longitude variations, weather variations, and atmospheric variations of the testing system relative to the measurement location [9]. In order to best account for these errors without adding excessive complexity to the process, it is imperative to use the solar flux measurements from the correct space weather index on the NOAA website. Usually the index that is nearest to the location of the ground station is the one utilized. The space weather index used for the NPS ground station is Sagamore Hill, MA. Despite the slight variations in measured solar flux at the NOAA site compared to the MC3 ground station location, such differences are considered negligible for the purposes of the G/T analysis [9].

3. Wavelength (λ)

Wavelength is a function of frequency and is a simple conversion using Equation 6 [9]:

$$\lambda = \frac{c}{f}, \tag{6}$$

where

λ Wavelength of the measurement frequency in meters

c Speed of light (299, 792, 458 m/s)

f Measurement frequency in Hertz (Hz)

4. Correction Factor (C)

The solar disk has an angular diameter of about one degree, and the S-band parabolic dish used by the NPS ground station is about three degrees. The pointing accuracy of the S-band dish is about 0.1 degrees. From the parabolic dish's perspective, the sun does not appear as a single-point RF source. This means that it is difficult to pinpoint the center of the sun, because the RF signal could be from the outer third, the middle third, or anywhere in between. In such cases, the RF signal would be slightly reduced, as the antenna would not be collecting it in the antenna's peak direction. Ultimately, taking measurements without accounting for these factors results in inconsistencies. In order to account for those errors, the beam correction factor, Equation 7 is used [11], [5];

$$C = \frac{1 - \exp\left(-\left(\frac{r}{B_w}\right)^2 \times \log_{10}(2)\right)}{\left(\frac{r}{B_w}\right)^2 \times \log_{10}(2)}, \tag{7}$$

where

C Beam Correction Factor

r Effective RF diameter in degrees

B_w Antenna Beam width in degrees.

The effective RF diameter in degrees (r) is calculated using Equation 8 [9]:

$$r = B_{HPBW}\left[1.24 - 0.162\log_{10}\left(f_{GT}\right)\right], \tag{8}$$

where

r Effective RF Diameter in degrees

B_{HPBW} Half-power Beamwidth; apparent angular diameter in degrees

f_{GT} G/T measurement frequency in GHz.

B_{HPBW} is the apparent angular diameter of the object from an observer on the Earth's surface. When using the sun as the RF source, that value is 0.525 degrees [9].

The antenna beamwidth is measured in degrees and is a function of wavelength and antenna diameter [9].

$$B_w = 68\frac{\lambda}{D}, \tag{9}$$

where

B_w Antenna Beamwidth (degrees)

λ Wavelength (Hz)

D Antenna Diameter (m).

The results from Equations 8 and 9 are used in Equation 7 to determine the correction factor [9].

5. Attenuation (α)

Attenuation is the reduction of the power density of the RF source's electromagnetic waves as they propagate through space. Those losses can occur from a variety of factors, such as rain, elevation angle, barometric pressure, frequency, clouds, and atmospheric composition [9]. Multiple forms of attenuation can impact the RF power density. The two main forms that apply in this thesis are atmospheric and rain attenuation.

Atmospheric attenuation depends on elevation angle and frequency as shown in Equation 10 [12];

$$\alpha = 10^{\frac{-A_g/\sin(el)}{10}}, \tag{10}$$

where

α Atmospheric Attenuation at elevation angle

A_g One-way zenith attenuation through atmosphere

el Elevation angle (degrees).

A_g is 0.032 dB at S-band and corresponds to the one-way zenith attenuation (at 90 degrees) through the atmosphere [13]. To account for the attenuation at other elevation angles, A_g is divided by the sine of the elevation angle [13].

In addition, rain attenuation can significantly impact G/T calculation. However, the analysis of rain attenuation is complex and not within the scope of this research effort. Therefore, during this research, we avoided rainy weather.

C. ALTERNATIVE METHODS TO CALCULATE G/T

There are a number of RF sources that can be used for the G/T calculation. This section explains a couple of the alternative sources, demonstrates the complexity of the calculations involved to use the moon as an RF source, and why the sun is the preferred RF source for this research.

1. Moon

To utilize the moon as an adequate RF source for G/T calculations, the system must be relatively larger in size, because smaller aperture antennas will not have enough P_{delta} for a useful G/T [9]. The correct combination of frequency band and antenna size must be used in order to obtain a usable G/T, shown in Figure 1 [9].

	Frequency Band					
Size	L	S	C	X	Ku	Ka
1.5 m (5 ft.)	x	x	x		✓	✓
1.8 m (6 ft.)	x	x	x		✓	✓
2.4 m (8 ft.)	x	x		✓	✓	✓
3.0 m (10 ft.)	x		✓	✓	✓	✓
3.7 m (12 ft.)		✓	✓	✓	✓	✓
5.0 m (16.4 ft.)		✓	✓	✓	✓	✓
x	Unable to accurately measure at given frequency					
	Accurate measurement "may be" possible					
✓	Able to accurately measure at given frequency					

Figure 1. Ability to Use Moon as RF Source to Measure G/T Based on Antenna Size and Frequency Band

One limitation of using the sun to calculate G/T that the moon can overcome, is access to the sun as an RF source at locations near the poles. At those high latitudes, there are periods of several weeks to months when the sun cannot be accessed. The sun's unreliability at those latitudes renders it unusable, and at those locations, an alternative source of RF is required to monitor the health of ground stations; the moon is that reliable alternative.

That said, although the moon can be accessed at certain latitudes where the sun cannot, there are many variables that must be accounted for when using the moon as the RF source. Those variables include flux density, the moon's phases, its extended size, and its time-varying distance from earth [14].

a. Lunar Flux Density (L_0)

This variable is substituted for the solar flux density in the G/T equation if the moon was chosen as the RF source. Unlike the solar flux density, this computationally intensive variable must be calculated on station, because there is not a database of measurements to utilize for interpolation. Lunar brightness temperature, angular diameter of the moon, and measurement frequency are the variables that must be accounted for to obtain an accurate calculation [14]. The accuracy of the calculation is generally much higher than if the sun was the RF source, because the moon is a much less volatile radiator. Using Equation 11,

the ground station can compute the value of the lunar flux density within +/-4.34 percent accuracy [9]:

$$L_0 = 7.349 f^2 T d^2 , \quad (11)$$

where

L_0 Lunar Flux Density in Jansky's (10^{-26} W/Hz/m^2)

f G/T measurement frequency in GHz

T Average Lunar Brightness Temperature in kelvin

d Angular Diameter of the moon in degrees.

The accuracy of the lunar flux density equation can be increased to within 1 percent certainty if the variation of the solar insolation at the lunar surface caused by the Earth's eccentric orbit is factored in; however, for the purposes of calculating G/T, this level of precision is not necessary [9].

Within equation 11, the average lunar brightness temperature (T) is a function of lunar phase angle, measurement frequency, and lunar phase lag. Equation 12, published by the National Bureau of Standards, is used to calculate the average lunar brightness temperature within +/-0.18 percent accuracy [9]:

$$T = T_0 \left[1 - \left(\frac{T_1}{T_0} \right) \cos(\phi - \psi) \right], \quad (12)$$

where

T Average Lunar Brightness Temperature, Kelvin

T_0 $207.7 + \frac{24.43}{f}$

$\frac{T_1}{T_0}$ $0.004212 f^{1.224}$

f Measurement Frequency in GHz

ϕ Lunar Phase Angle in degrees (0 at New Moon)

ψ Lunar Phase Lag in degrees = $\frac{43.83}{1+0.109 f}$.

The average temperature is used rather than calculating the true value, because the latter would require compensating for solar radiation changes, orbit shifts, distance variations between the sun, moon, earth, and lunar surface composition; all of which is unnecessarily complex to calculate a reliable G/T. [9].

Equation 13 is used for calculating phase angle to a high degree of accuracy [9]:

$$\phi = \tan^{-1}\left(\frac{R\sin\psi}{\Delta - R\cos\psi}\right), \tag{13}$$

where

ϕ Lunar Phase Angle in degrees

R Geocentric Distance from earth to the sun in km

Δ Geocentric Distance from earth to the moon in km

ψ Geocentric Elongation of the moon.

Similar to the sun, when determining the angular diameter of the moon, it is the apparent lunar diameter when observed from the Earth's surface using Equation 14 [9]:

$$d = \frac{0.5182}{\frac{r_0 / a}{60.268} - 0.0166\sin(el)}, \tag{14}$$

where

d Angular Lunar Diameter in degrees

r_0 Geocentric Earth-Moon Separation in km

a Equatorial Radius of the Earth in km (6378.1366 km)

el Elevation Angle of the Lunar Center in degrees.

Solving for Equations 12, 13, and 14 will determine all the variables needed when solving for the lunar flux density. Once the lunar flux density is solved for, and that value is multiplied by 10^4 to obtain the units of SFU (10^{-22} W/Hz/m^2), the only other difference between using the sun or the moon is the source of RF. When using the moon, the parabolic dish points at and collects the RF from the moon and cold sky to obtain the *y*-factor. Otherwise, the rest of the G/T process mimics that of using the sun. There are several more equations used to calculate the geocentric distances and elongation to determine the position of the moon [9]. However, for the purposes of this thesis, the equations are provided to help develop an understanding of the context and computational intensity required when using the moon as the RF source when compared to the sun.

While the moon's location and flux density can be mathematically intensive to calculate, if that is not a concern for the ground station, a moon-based G/T has the potential to be more accurate than a sun-based calculation. This improved accuracy is based on the certainty provided from the lunar flux density calculation when compared to a solar flux measurement [11]. The lunar flux density value is obtained by taking the moon's radiation as a stable black-body radiation, and representing it as a disk of uniform brightness. The averages of brightness temperature, lunar phase, and lunar angular diameter, as seen from the antenna site at the time of the measurement, are used for this representation [11].

The moon as an RF source provides stable radiation flux density and minimal uncertainty. Its accuracy and efficacy has led to its adoption by the European Space Agency for use with apertures ranging from seven to thirteen meters [11]. However, using the moon as the primary source of RF requires larger antennas at higher frequencies and a computationally intensive calculation to be performed at the ground station.

2. Radio Stars

Another RF source that can be used to calculate the G/T is a radio star. This research does not use a radio star as the primary source of RF. The ground stations in the MC3 network do not use antennas large enough to produce the minimum G/T required to collect the faint RF signal produced by a radio star. A radio star is a stellar object that can produce significant RF emissions [2]. Calculating the G/T using a radio star entails the exact same method as using the sun or moon, except that the parabolic dish collects the RF (P_{source}) from the designated radio star instead, and a well-defined flux density equation for the specific radio star is required [2].

A major disadvantage that limits the usage of radio stars as the RF source is that the ground station must have an inherent G/T substantially greater for radio stars than for applications involving the sun, or local emitters [2]. The minimum G/T required is determined by the strength of the RF being emitted from the radio star. No two stars emit the same RF, and if the RF emitted is weaker, a greater G/T value is required from the ground station in order to collect the signal [2]. For example, it is estimated that in order to use the radio star Cassiopeia A, the G/T required from a ground station is at least 35 dB/K, which is more than ten times greater than that required to use the sun [2]. Radio stars can work as the RF source for larger ground stations, but for the NPS ground station, where the G/T is in the 5–13 dB/K range, utilizing radio stars is not feasible. Considering all of the methods described for calculating G/T, the next section discusses the motivation for using the sun as a suitable RF source.

D. SUN

There are pros and cons for using each of the RF sources previously described. Using celestial bodies as the RF source for G/T calculations is most common because they are visible for extended periods of time at most ground station locations [9]. Whereas, again, there are locations in extreme latitude regions where the sun may not be visible for weeks at a time, rendering the sun useless for the purpose of calculating G/T [9]. Another limiting factor is the size of the parabolic dish that is used. For larger dishes (greater than ten meters), radio stars are a possible source of RF. However, for smaller dishes (less than

five meters), the only other reliable source of RF is the moon [9]. The NPS ground station is not located in an extreme latitude region, but it does have a smaller dish that limits the available RF sources to calculate G/T to the sun and the moon.

One of the advantages of using the sun is that almost any system can use it as the source of RF to calculate G/T; as long as the dish is bigger than 1.5 meters, and the frequency is L-band and greater (1–2 GHz) [9]. The moon is a much weaker source of RF, and requires larger antennas at higher frequencies than are used in this research, in order to be used for G/T calculations [9].

While NPS is capable of utilizing either the sun or the moon as the RF source, it is much easier to begin this process with the sun and transition to the moon as an alternative, thus allowing for greater flexibility. There are several reasons why it makes more sense to initially master using the sun even if other sources can be used. First, the solar flux calculation done by NOAA eliminates a process that would be computationally intensive to conduct at the ground station. This eliminates one variable that would otherwise need to be accounted for by the ground station operators. Second, in order to take the G/T measurement, the source must be accessible. For the moon, that would mean in the middle of the night. Logistically, and for the purposes of this thesis, conducting tests in the middle of the night would be another unnecessary challenge. The sun can be accessed in the middle of the day when there is maximum support available, and with less difficulty physically accessing the ground station. Moreover, at the beginning of this research, an autonomous process to calculate the G/T using the sun was already in development.

Once NPS can refine the G/T calculation utilizing the sun, it would make sense to then expand the capability to use the moon. Using the moon would open up the possibility to take the measurements during the night, and potentially minimize the interference with normal day-to-day operations of the ground station.

THIS PAGE INTENTIONALLY LEFT BLANK

III. METHODOLOGY

A. OVERVIEW

This chapter reviews the technique to measure G/T using the sun as the source of RF and then examines the S-band G/T measurement technique that is conducted at National Space Agency, Malaysia (ANGKASA) and how it compares to the work in this thesis. Then we explain what the theoretical G/T and practical G/T are, and what role those values have in this thesis, along with a more detailed explanation of the configuration of a link, to better understand the factors involved in a G/T measurement.

B. ASSESSMENT OF THE SOLAR NOISE TECHNIQUE FOR MEASURING G/T

Griffiths and Libert assess the method of using the sun as the RF source, and comparing it to the RF output from the cold sky to obtain a G/T value [3]. This method is relatively simple when compared to some of the previously mentioned methods, but at the time of Griffits and Libert's analysis in 1994, this was an obscure approach. Therefore, Griffiths and Libert set out to determine the achievable accuracy of using the sun as the source of RF for the G/T calculation, and to identify and catalog critical aspects of this measurement [3].

One of the first complications they observed during their research was the uncertainty of the solar flux. In 1994, this was a much more challenging task. However, there was an observatory taking the solar flux measurement, the Penticton Radio Observatory, in British Columbia, Canada, which they used in their research. A measurement of the Solar Flux was taken by the Penticton Radio Observatory daily at a frequency of 2.8 GHz, and could be readily and reliably obtained by Griffiths and Libert [3].

A second issue was the water vapor and precipitation attenuation impacting the Solar Flux. The conclusion reached by Griffiths and Libert was to avoid this factor impacting the measurement completely, by taking this measurement on a clear, dry day [3].

The last issue that needed to be overcome in the Griffiths and Libert study was the pointing accuracy of the antenna. Griffiths and Libert concluded that unless a sophisticated pointing mechanism is used to enable the antenna to be pointed accurately at the sun, the error will be greater than 1 dB [3].

Ultimately, Griffiths and Libert stated that even with the variety of complications resulting from using the sun as the RF source, it is extremely useful for estimating G/T to an accuracy of greater than +/- 1 dB. They further suggested that the remaining complications they identified could be further mitigated, and that this method could yield an even more accurate result [3].

Each of the concerns mentioned in Griffiths and Libert's research have been considered for this research with the following solutions. The Solar Flux measurements are readily available on the NOAA website at several locations and frequencies that make it easy to use the interpolation equation, Equation 4, discussed in Chapter II. We have reached the same conclusion with regard to rain attenuation, and do not conduct measurements in poor weather conditions. Lastly, NPS utilizes a sophisticated antenna pointing capability to mitigate any errors associated with pointing inaccuracies. Griffiths and Libert did not look into the feasibility of conducting this measurement with any consistency, or making the process automatic by developing a tool for assessing the health of a ground station. However, Griffiths and Libert's research does reinforce the idea that G/T can be conducted accurately and reliably with the sun as the source of RF.

C. A REVIEW OF S-BAND ANTENNA SYSTEM G/T MEASUREMENT TECHNIQUE (ANGKASA)

This research adapts ANGKASA's S-band antenna system measurement technique with slight variations. The S-band antenna operating at ANGKASA is used for tracking, telemetry, and control (TT&C) [13]. The antenna also has the capability to communicate with low earth orbit (LEO) and middle earth orbit (MEO) satellites. The antenna specifications utilized at ANGKASA are similar to the S-band antenna used at NPS, although with subtle differences. The uplink and downlink frequencies at which the antennas operate are identical, 2025–2110 MHz and 2200–2290 MHz, respectively.

However, the antenna ANGKASA uses is 5 meters with an overall positioning accuracy of .005 degrees compared to the 3 meter dish with 0.1 degree pointing accuracy at NPS [7], [13].

ANGKASA's process of measuring the collected RF from the sun and cold sky to obtain the value for the *y*-factor is similar to the method used in this thesis, with some important differences. ANGKASA only measures a single frequency in the S-band, 2200 MHz, for their research [13]. Using that frequency, ANGKASA measures the RF signal peak amplitude of both the sun and cold sky three separate times, and records the three peak values for each. Once the peak values are obtained, ANGKASA averages those values. The averages of the peaks for the sun (P_{sun}) and cold sky (P_{coldsky}) are used to calculate the P_{delta} and ultimately the *y*-factor [13]. In this thesis, rather than a single frequency, we collected a much larger sample size, which will be discussed in more detail in Chapter IV.

In addition, this thesis calculates the solar flux value using the same method as ANGKASA: it is interpolated from the NOAA recorded values. All of the errors are accounted for using the same method, with one exception: ANGKASA applies an estimated test measurement error of 0.5 dB to their G/T equation, while for this thesis that value is not applied [13]. Rather, all significant errors are accounted for, as will be discussed in more detail in Chapter IV.

Moreover, ANGKASA only collects the RF for a single frequency. In this thesis, the purpose is to collect the RF data of a frequency range from 2200 MHz to 2300 MHz; therefore, we collect and record multiple RF measurements in the various frequencies. This will be outlined and explained in greater detail in Chapter IV. Collecting three peaks of the sun and cold sky, and averaging the values to determine a single P_{delta} appears to be a sufficient sample size for a basic G/T at a single frequency. However, this method does not account for much of the context that this thesis is aiming to capture in this process. One example of this possibility is the situation wherein the ground station could be experiencing interference with RF collection at 2250 MHz, while experiencing normal results at 2200 MHz. Utilizing ANGKASA's method, that interference would go unnoticed. The context

of collecting this data at various frequencies will also be discussed in greater detail in Chapter IV.

The ANGKASA paper demonstrated that G/T is an important performance indicator to ensure a reliable communication link between ground stations and satellites. In the future, a comparison between the various methods used to calculate the G/T of similar systems should be conducted to provide additional context [13]. This thesis seeks to address the comparison of G/T between multiple ground stations in the MC3 network.

D. THEORETICAL G/T VS. PRACTICAL G/T

In this thesis, a theoretical G/T value is calculated for the MC3 system at NPS. After this value is calculated, this theoretical value is compared to a practical value using data collected from a sun vs. cold sky measurement to obtain a G/T with the MC3 system. In order to calculate the theoretical G/T, it is important to understand the configuration of a link and the derivation of the theoretical G/T equations.

1. Configuration of a Link

In a normal link configuration, there are two sides: the transmission side and the receiving side [15]. On the transmission side, a transmitter (T_x) is connected by a feeder to the transmit antenna. The transmit antenna has a gain (G_T) in the direction of the receiver. Equation 15 describes the power (P_T) radiated by the transmitter toward the receiver, which is the effective isotropic radiated power (EIRP) [15].

$$EIRP = P_T G_T \ , \tag{15}$$

where

$EIRP$ Effective Isotropic Radiated Power

P_T Transmitted Power

G_T Transmitted Gain.

On the receive side, the signal interacts with the receive antenna with gain (G_R) in the direction of the transmitter, followed by the feeder leading to the receiver (R_x) [15]. Figure 3 represents the various elements that participate in a link [15].

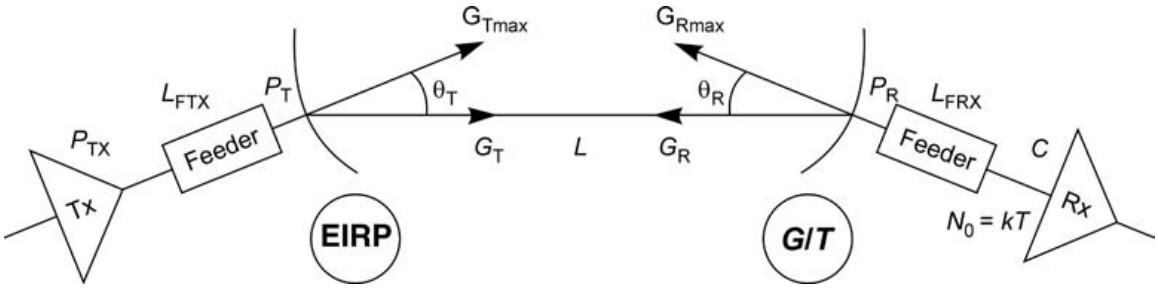

Figure 2. Configuration of a Link.

As Chapter II discusses, there are losses experienced throughout this link that affect the quality of the signal received. For the purposes of this thesis, the sun and cold sky would be acting as the "transmitter" on the left side of Figure 2, and the MC3 ground station as the "receiver" on the right side [15]. The MC3 ground station is measuring the RF signal strength from both the sun and cold sky to calculate a *y*-factor that is used in the G/T equation (Equation 1). The following sections explain the derivations used for the theoretical gain and noise temperature.

2. Gain (G)

Antennas are not perfect spheres; if they were, radiation would occur perfectly in every direction. The gain of an antenna is a number that describes the ability of the antenna to radiate more or less in any direction compared to a theoretical antenna, also known as an isotropic antenna [15]. For the antenna collecting the RF, or the receive antenna, the gain describes the ability of the receive antenna to collect the RF compared to the isotropic antenna. In an ideal scenario, the gain, or G_{max}, has the value given by Equation 16 [15]:

$$G_{\max} = (4\pi / \lambda^2) A_{eff} \,, \tag{16}$$

where

$G_{\max}$ Maximum Gain

λ Wavelength (m)

A_{eff} Effective aperture area of the antenna.

The effective aperture area of the antenna is the area of the dish multiplied by the efficiency of the antenna. The efficiency (η) of the antenna accounts for several factors such as spill-over loss, surface impairments, ohmic and impedance mismatch losses, and illumination law [15].

$$A_{eff} = \eta A \,, \tag{17}$$

where

A_{eff} Effective aperture area of the antenna

η Efficiency of the antenna

A Area of the antenna.

Using Equations 16 and 17 for a given antenna will establish the theoretical maximum gain. Next, we examine the system noise temperature.

3. System Noise Temperature

To derive the theoretical value of the system noise temperature, both the antenna noise temperature (T_A) and the receiver noise temperature (T_{eRX}) must be considered [15].

The antenna noise temperature (T_A) is a function of atmospheric conditions, of elevation angle, and of the frequency [15]. As Chapter II discussed, rain attenuation impacting atmospheric conditions can be neglected due to the fact that measurements were

only taken in “clear sky” conditions. The remaining contributions to noise temperature of an antenna in clear sky conditions are from the ground and sky, as depicted in Figure 3 [15].

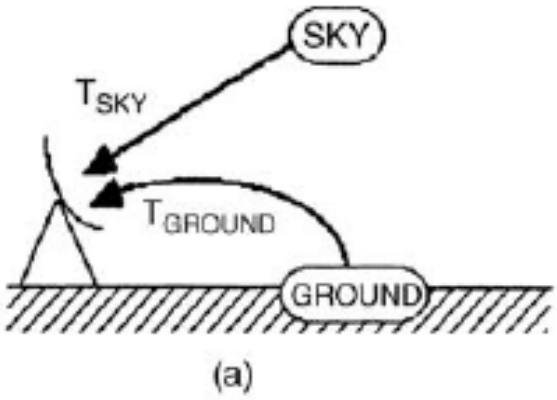

Figure 3. Contributions to the Noise Temperature of the Antenna in Clear Sky Conditions

To account for the effects on antenna noise temperature of elevation and frequency, a noise power spectral density chart is used [15]. Figure 4 is the noise power spectral density chart that displays the noise at the receiver, while accounting for frequency and elevation angle [15].

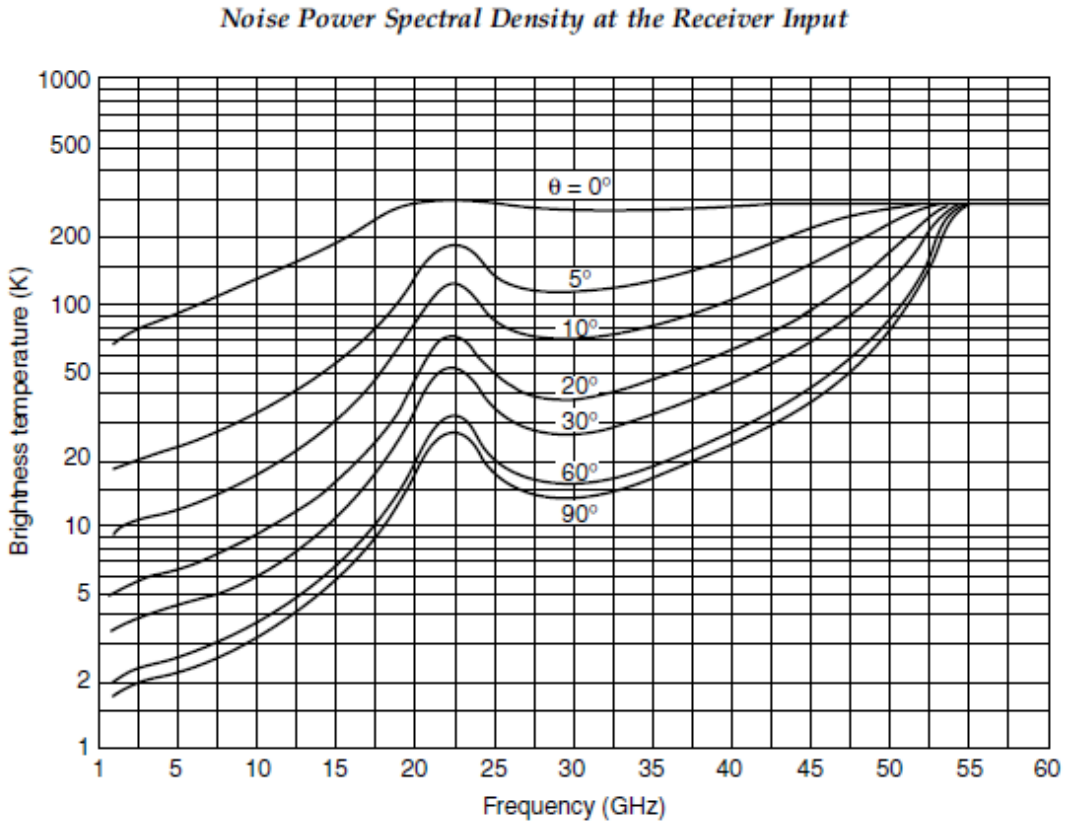

Figure 4. Brightness Temperature of Clear Sky as a Function of Frequency and Elevation Angle

Combining the noise contributed from the clear sky and brightness temperature from the elevation angle of the antenna yields the overall temperature of the antenna [15].

Next, we must consider the receiver noise temperature to combine with the T_{eRX} to determine the overall system noise temperature. Once the signal is collected by the antenna, it passes through a variety of cables and equipment, known as the RF terminal, until the data arrives at the equipment being used to measure the RF signal [15]. For the purposes of this thesis, the collection equipment being used is the USRP and the FieldFox. The RF terminal consists of a low noise amplifier (LNA), filters, splitters, switches, relays, and up and down converters, all of which are connected by cables. A simplified version of the RF terminal used at NPS is pictured in Figure 5 [5].

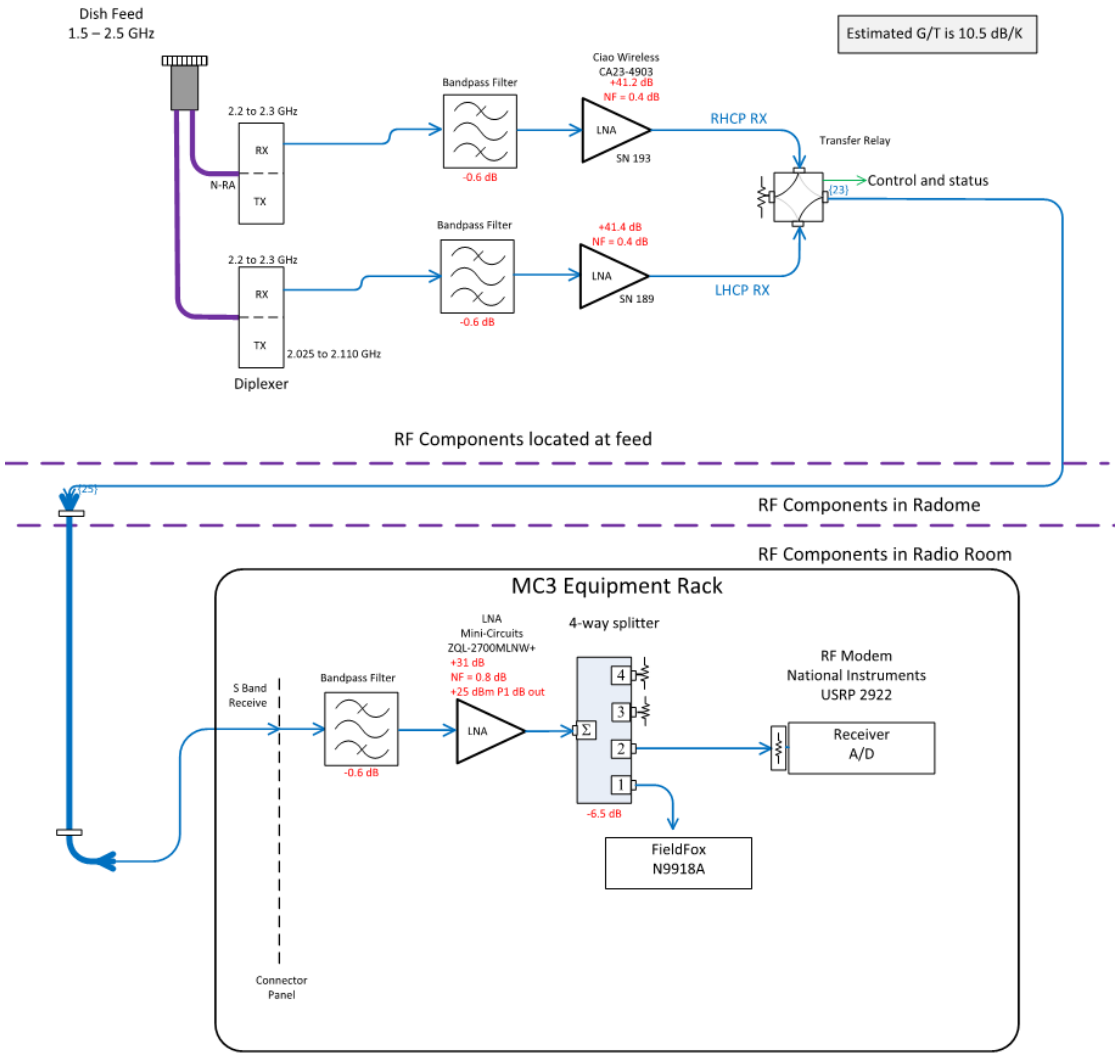

Figure 5. Simplified Version of the RF Terminal at NPS

Each piece of equipment and cable imperfection introduces noise that degrades the signal collected. An important part of the RF terminal to understand is the LNA, because it is used to amplify the received signal to much higher power values without degrading the underlying signal [15]. The tradeoff for the increased signal strength provided by the LNA is that it also contributes the most noise to the receiver noise temperature. The reason for this increased noise is that, while it amplifies the underlying signal, it also amplifies any noise that is present in that signal. Additionally, the noise in any signal continually increases as the signal travels through the RF terminal, which is likewise amplified by the

LNA. Therefore, it is imperative to place the LNA as close as possible to the antenna on the receive side to maximize the signal strength, as demonstrated in Figure 5 [5].

Another loss experienced in the RF terminal is due to the feeder. Figure 6 demonstrates the cascading effect of the losses experienced by the signal, and the variables used to account for them in Equation 18.

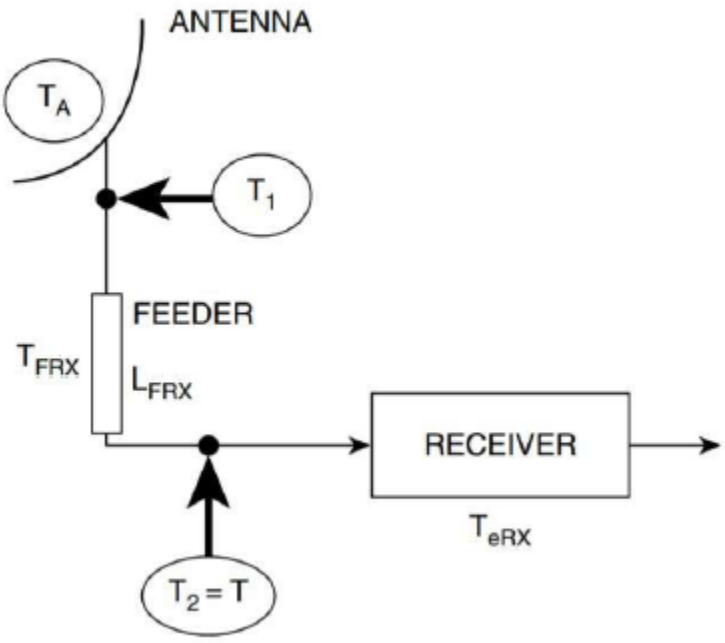

Figure 6. A Receiving System. Source: [15].

T_1 represents the sum of the noise temperature (T_A), feeder, and receiver shown in Figure 6 [15]. The value for the noise temperature of the feeder (L_{FRX}) can be derived from Figure 7.

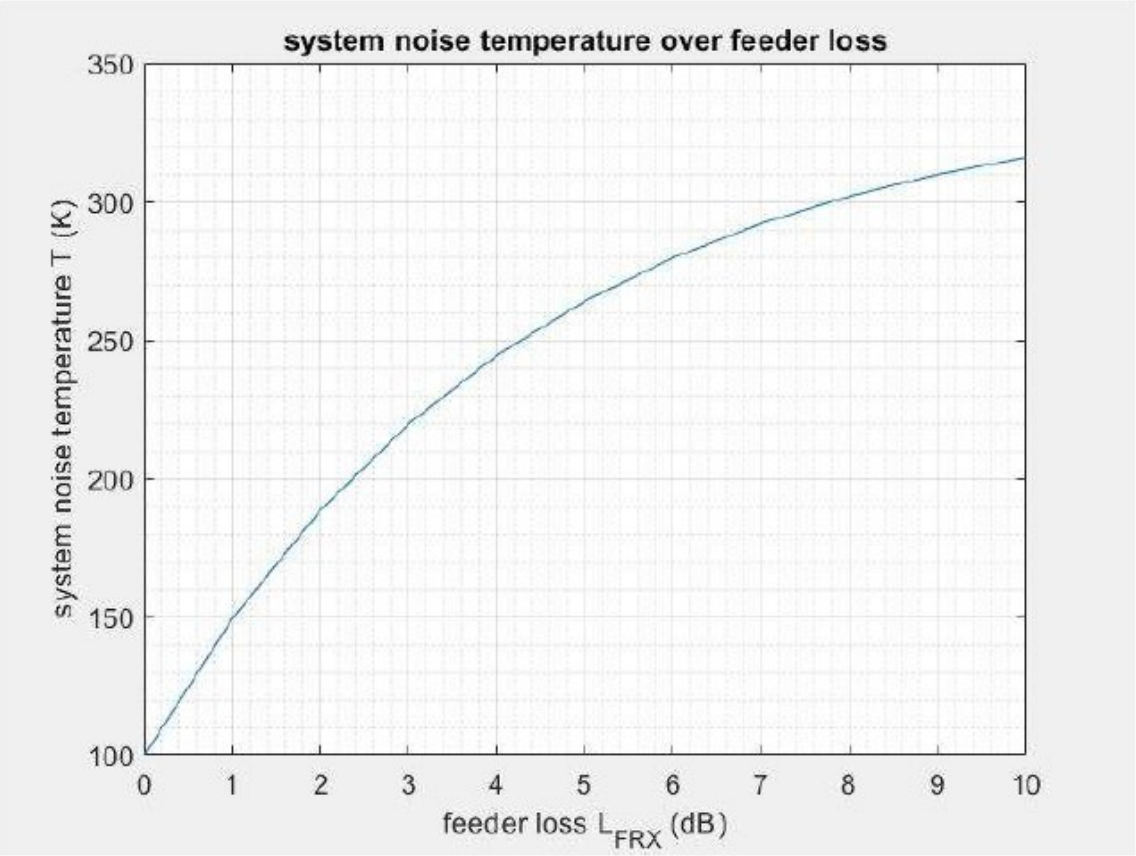

Figure 7. Feeder Loss Based on the System Noise Temperature. Source: [15].

T_2 in Equation 18 represents the system noise temperature, which accounts for all of the noise generated by the antenna, feeder, and receiver [15]. The combination of noise from the sources listed comprise the system noise temperature, *T*. The formula for system noise temperature accounting for all of these factors is demonstrated in Equation 18 [15]:

$$T_2 = T_1 / L_{FRX} = T_A / L_{FRX} + T_F(1 - 1/L_{FRX}) + T_{eRX} \quad (18)$$

where,

T_2 System noise temperature (K)

T_1 At the antenna output, before the feeder losses, temperature (K)

L_{FRX} Feeder attenuation losses (dB)

T_A Temperature at the antenna (K)

T_F Temperature of the feeder (K)

T_{eRX} Input noise temperature of the receiver (K)

All sources of noise in the RF terminal link contribute to the overall system noise temperature at the receiver input [15]. These factors represent those that must be accounted for, and for which the equations utilized, in order to independently measure the system noise temperature for the G/T value.

4. Theoretical G/T

We calculated the maximum theoretical value for G/T of the NPS ground station. The theoretical maximum value for the antenna gain can be derived from Figure 8 [15].

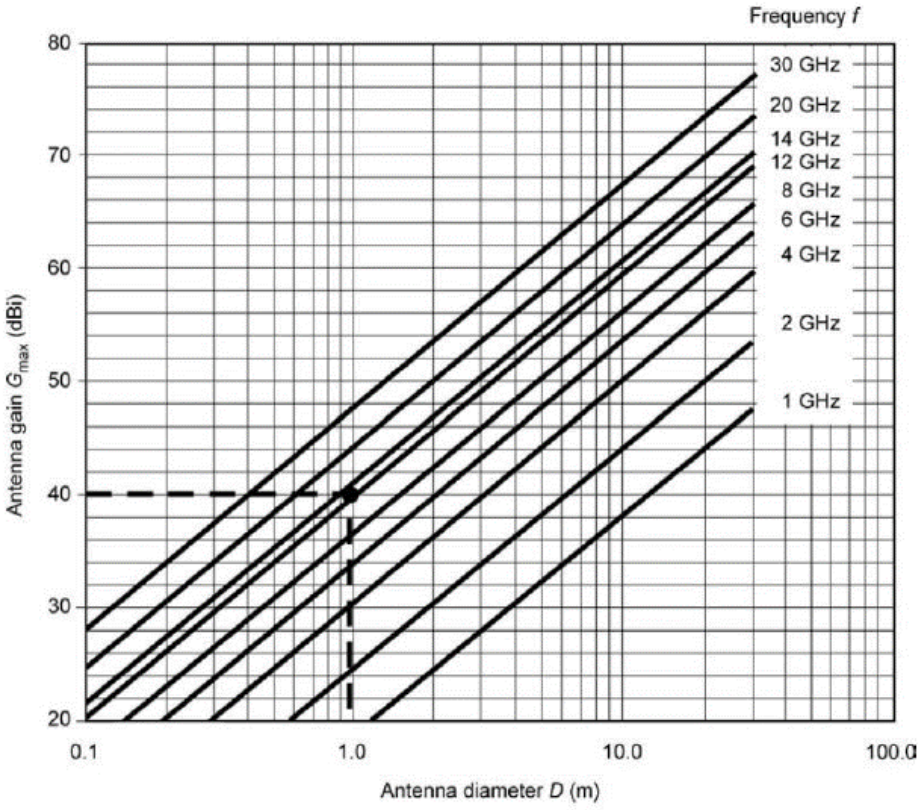

Figure 8. Max Antenna Gain Based on Antenna Diameter and Frequency

Using the NPS ground station values of 2 GHz for the frequency and 3 meters for the size of the antenna, the theoretical maximum gain is 34 dBi.

To calculate the theoretical system noise, Equation 18 is used with NPS ground station specific values. T_{eRX} is estimated to be 28 K, T_F is 290 K, T_A is 50 K, and to simplify the attenuation losses, the value used is estimated to be 1.25 dB [5].

The resultant theoretical G/T for the NPS ground station is 12.99 dB/K. What this value conveys is that in an ideal scenario, this is the highest G/T value achievable at this ground station. This serves as a baseline when calculating the practical G/T. The goal is to have the practical G/T value as close as possible to the theoretical value, because that demonstrates the ground station is operating at a high efficiency.

5. Plan of Action

This thesis is based on developing a method to automatically take all of the measurements required for a "practical" G/T. Before we share the results of a practical G/T calculation, let us outline where we started in the process of taking this measurement automatically, and how our results compare to the goal we made at the outset.

As we began, it was necessary to learn the details required for a proper G/T measurement, become familiar with the process currently being used, and sort the details required to achieve our goal of creating an automatic process for taking a G/T measurement. As we discussed earlier, the key processes that are involved with obtaining a G/T calculation are the ability to track the sun with the antenna, a way to collect the RF signal, as well as develop code that can process the RF signal collected, and a way to store the results.

At the beginning of this research, the ability to track the sun had been developed, and a FieldFox was being used to collect the RF signal. The code developed to process the RF signal the FieldFox collected was configured for the FieldFox specifically, and there was no database created to store the results. A key objective in this thesis was to utilize a USRP instead of the FieldFox for RF collection. A USRP would allow most of the MC3 ground stations to use the developed G/T process because they each already possess a

USRP. USRPs are much cheaper to acquire at $3,000, than the $80,000 FieldFox spectrum analyzers. Although using a USRP is a key mission of this thesis, when we started our research it had yet to be determined if a USRP was even capable of collecting RF signals with enough fidelity to produce a usable G/T value. Therefore, our goal was to utilize the USRP for RF collection to determine if it was adequate as an instrument for collecting a suitable G/T value.

SDL in Utah is a part of the MC3 network, and developed code called Titan that processed the RF signal collected by the USRP. SDL shared that code with NPS, and we began to analyze the underlying code. The purpose of evaluating this code was to see if this system was capable of extracting useful RF signal data that could be used for G/T calculations. The goal of this analysis was to determine if we could utilize this tool, thus saving time and resources, allowing us to turn our attention to other aspects of this endeavor.

Upon investigating the code provided by SDL, we concluded that it could be useful and warranted spending more time working with it. Time was then spent streamlining the code, retaining the useful elements, and removing the elements that added no value to our analysis. Our focus was exclusively on the elements of the code that could properly process the RF signal. The next step was to configure the SDL code that we manipulated, to integrate with the code developed prior to this thesis, by Bastian Beicher [4]. Once the SDL code was adjusted to be more efficient, and able to integrate with the NPS system, we then conducted operational tests and compared those results with the results being achieved by the FieldFox. Comparing the results obtained using the USRP and the new code to the results obtained using a FieldFox helped drive our efforts moving forward.

In order for this comparison to be useful, it was imperative to take the measurements using the exact same RF signal collected. A piece of equipment called a splitter (a device designed to divide a single RF signal into multiple signals, in our case two) was used to ensure a consistent RF signal was presented to each device. The results of this analysis helped us determine if the manipulated SDL code could be useful. The results of this analysis are shown and discussed in Chapter IV. After we produced G/T calculations from measurements with Titan, a bigger sample size was collected, and

additional modifications were made to the underlying code, which is also discussed in Chapter IV.

The final significant milestone was collecting sun and cold sky measurements from multiple ground stations in the MC3 network remotely from the NPS ground station. The measurements collected were used to generate G/T values for the ground stations, and those results are also discussed further in Chapter IV.

6. Practical G/T

For the practical G/T calculation, rather than measuring G and T individually, all of the other variables are measured and calculated in Equation 1. The results from the practical G/T calculation, and a comparison to the theoretical G/T are discussed in Chapter IV.

THIS PAGE INTENTIONALLY LEFT BLANK

IV. EXPERIMENTAL RESULTS

In this chapter we finish the discussion of theoretical versus practical G/T, walk through the results produced throughout this thesis, and discuss the decisions made that drove our analysis, and conclusions reached from the actual results. Finally, I present where we are in the process of creating an automatic assessment of ground station health.

A. PRACTICAL G/T RESULT AND COMPARISON TO THEORETICAL G/T

A sun and cold sky measurement taken on 05 February 2021, when observing the values at 2.25 GHz, yielded -58.2 dB for the cold sky and -65.6 dB for the sun. The P_{delta} was 7.33 dB with the resultant y-factor of 5.41. This y-factor combined with the rest of the variables in Equation 1 led to a practical G/T value of 11.3 dB/K.

With a practical G/T value of 11.3 dB/K and a theoretical G/T value of 12.99 dB/K, the measured efficiency at this time would have been approximately 86.6%. While this individual efficiency value is useful, more context is needed to truly grasp a better understanding of how the ground station is operating.

To more fully understand the health of the ground station, one must first understand the normal or expected efficiency of that ground station. It is only when we understand the actual efficiency value, that we can understand the significance of the value we calculated, and whether or not further examination of the ground station is warranted. The only way to determine the "normal" efficiency of a ground station is to collect a much larger sample size. That larger sample size refers not simply to the number of observations made, but it should also include a wider range of frequencies in the 2.2 to 2.3 GHz range, not just a single frequency. Moreover, this evaluation also requires a large number of observations made over a protracted period of time—for example, observations over the course of several days to a few weeks. The better the sample size, the better we can "normalize" the health of that particular ground station.

B. RESULTS

When inspecting the code from SDL to see how the RF signal was parsed, there were several graphs and outputs produced from the code. These outputs are used to determine if it was worth spending time trying to implement all or part of the code into the overall process. The following graph demonstrates one of the ways the SDL code parsed the RF signal that was collected. Figure 9 shows shades of red that represent the strength of the RF signal being collected; time value in milliseconds is represented on the y-axis, and frequency of 400 kHz on the x-axis.

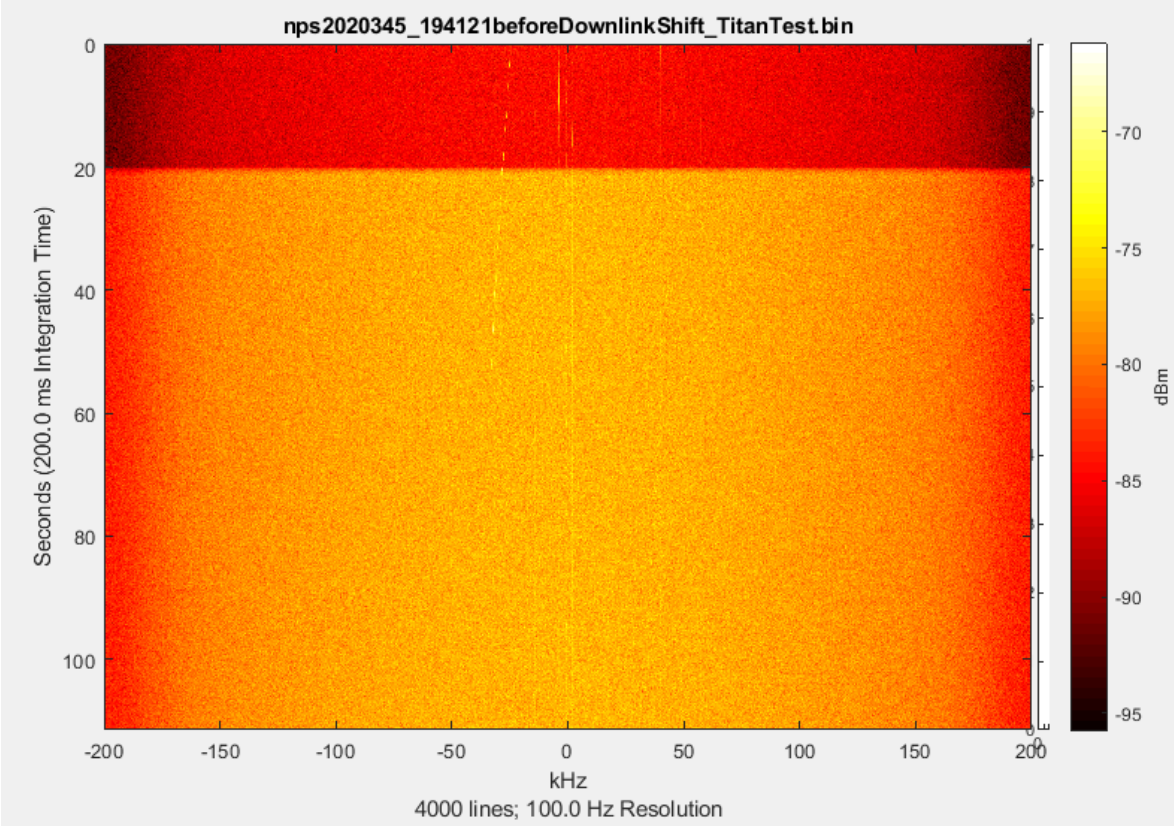

Figure 9. SDL RF Signal Strength Output at 2.25 GHz in dBm over 200 ms

Figure 9 clearly shows the antenna's progression as it moved into position and pointed at the sun. The abrupt shift of dark red/orange into a much lighter shade of orange/ yellow signifies the stronger RF signal being received, which is a visual representation of

the moment the antenna was "looking" at the sun. While this specific output from the SDL code was not used in this thesis, it provides an interesting visual representation that highlights the dramatic difference in RF signal strength when looking at the sun compared to the cold sky. It also provides more evidence demonstrating how valuable the sun can be as a resource for calculating the G/T.

Figures 10 through 15 display the graphs produced from both the FieldFox and Titan, collected from the same RF signal. While the RF signal was collected through different means (FieldFox and Titan), the same software was used to process and produce the various graphs. The software used was Matlab. Figure 10 shows the FieldFox sun (blue) and cold sky (orange) RF collections and their respective power in dBm over a 100 MHz frequency range, 2200 MHz to 2300 MHz (or 2.2 to 2.3 GHz).

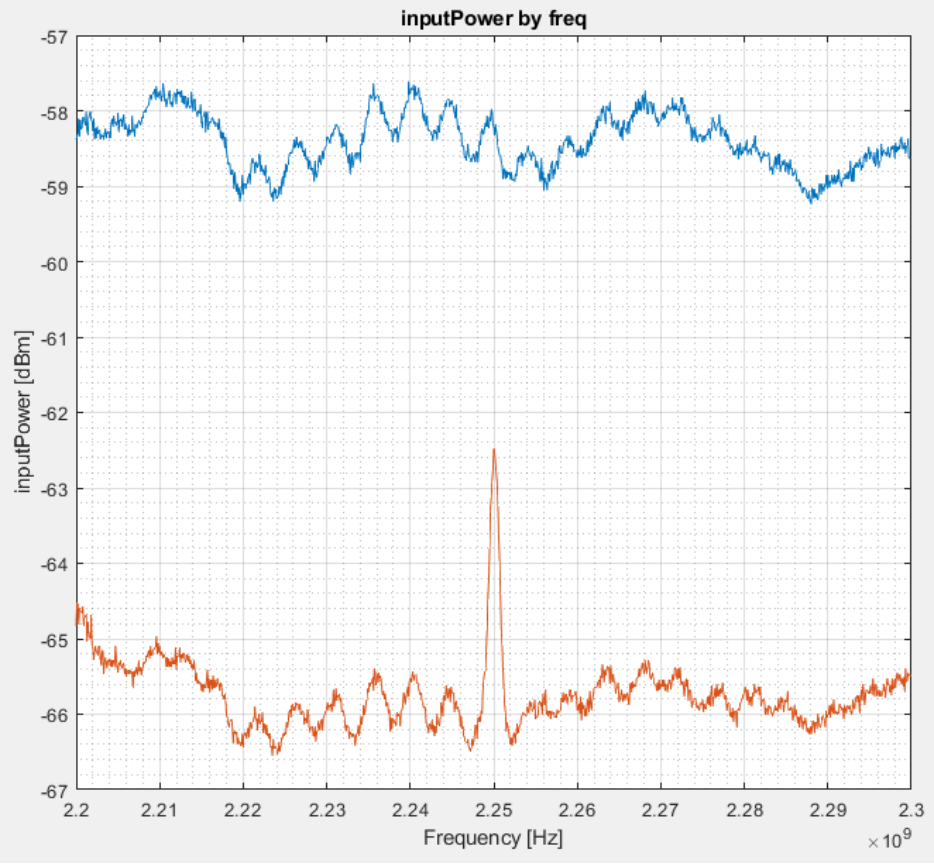

Figure 10. FieldFox Sun vs. Cold Sky Input Power from 2.2 to 2.3 GHz (100 MHz span)

The FieldFox was configured to take 1001 samples over a 100 MHz span. The frequency range of 100 MHz is ideal because it produces a graphical representation that clearly shows areas of interference or a potential degradation. Such interference is observed at 2.25 GHz in Figure 10. Figure 11 shows the resultant G/T for the measurements collected in Figure 10.

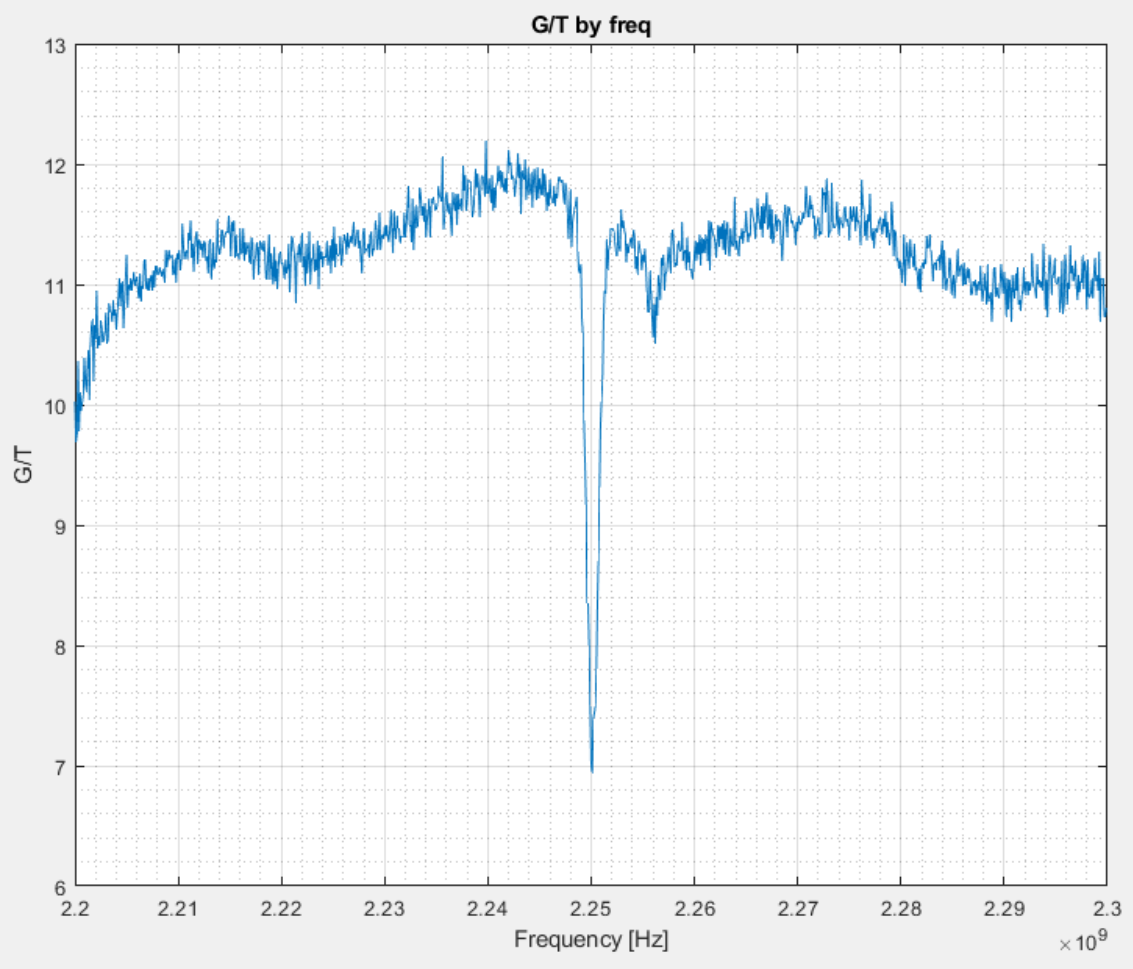

Figure 11. FieldFox G/T from 2.2 to 2.3 GHz (100 MHz span)

That spike or significantly decreased RF power received from the cold sky at 2.25 GHz had a significant effect on the G/T. A decrease of more than 4 dB/K was calculated and can be seen in Figure 11. Because the dropoff is so pronounced at the specific frequency of 2.25 GHz, the result suggests interference exists at that frequency. The most

likely source of interference was another entity actively communicating at that frequency. This result was unexpected, and interference of that magnitude could have significantly degraded communications with the NPS ground station.

If this interference occurred while a satellite was attempting to communicate with NPS over S-band, it could result in a decreased transfer rate as well as a reduced amount of data transferred. Absent a health check like the G/T method that produces graphs like Figure 11, or stored values of the G/T in a database, it is likely that an analysis of this observation would suggest that a resultant failing piece of equipment caused the measured degradation.

However, with this G/T method at our disposal, a cursory measurement can be taken to inspect any potential issues with the RF chain, or configuration of the link (demonstrated in Figure 3) before suffering through the arduous process of troubleshooting equipment. In this example, any investigation would likely fail to find a solution. However, if the G/T calculation looked something like Figure 11, then the focus could shift toward determining the source of that interference. Since there is a regulated list of users for each frequency band, the G/T process could be used to help ensure the right people are accessing the frequency band and help the users cooperate more efficiently to avoid degradation for all involved.

Unfortunately, we were unable to pinpoint the source of the specific interference. However, collecting the signal and displaying tangible results to display the data showcases exactly how useful and important the ability to take the G/T automatically can be.

The capability of the FieldFox to produce a G/T graph of this fidelity was not a surprise because this had already been established with previous work [4]. The purpose of using the FieldFox and recording measurements in this thesis is to compare a known result with the new method, the USRP Titan.

Figure 12 shows Titan's collection of sun and cold sky measurements that look similar to the FieldFox collection in Figure 10. Sun measurements are in blue and cold sky measurements are in orange.

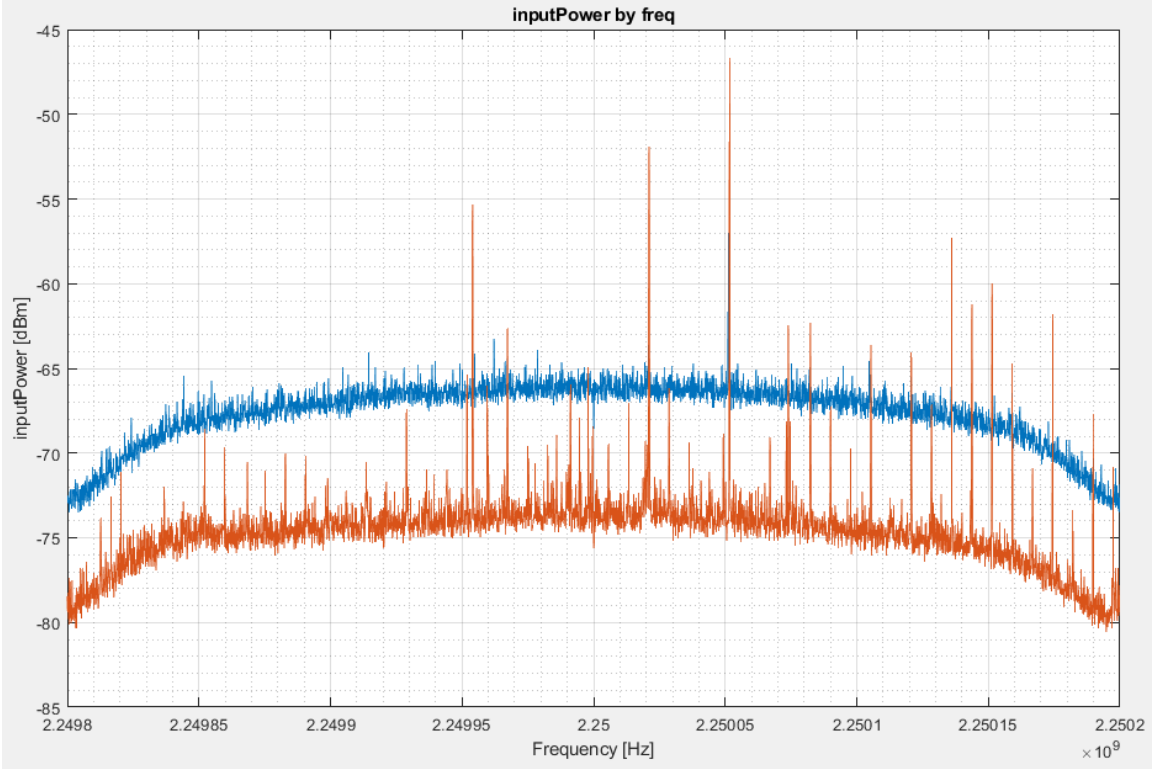

Figure 12. Titan Sun vs. Cold Sky Input Power from 2.2498 to 2.502 GHz (400 kHz span)

A major difference to note is the frequency span collected by the Titan is much smaller; instead of the 100 MHz (2200 MHz to 2300 MHz) that the FieldFox is capable of collecting, the Titan collected a much smaller sample of 400 kHz, or 2249.8 MHz to 2250.2 MHz. The sample size collected by the Titan is 4000 points instead of the 1001 of the FieldFox. The increased sample size of the Titan over a much smaller frequency range means more volatility in the RF collected. The volatility makes it harder to note more precise observations regarding the health of the antenna over the entire RF spectrum.

Ultimately, the goal is to produce a method that can observe the entire 2200–2300 MHz frequency range, due to the important observations regarding the antenna's health as displayed in Figure 11. It is also important to note that the bigger sample size of the Titan takes longer for the ground station to process and yield results. Processing duration was not a major concern for this thesis. Our focus instead was to create a reliable process to automatically calculate the G/T with the Titan. The duration to collect sun and cold sky

measurements combined with the processing time to calculate the G/T will become a factor as the network grows and services additional users. As the number of users a ground station services grows, the less time there is available to conduct the G/T calculation; therefore, maximizing the speed will become increasingly important.

Another anomaly that was observed, is the difference in relative RF signal strength received between the FieldFox and Titan. If both are collecting the same RF signal, the expected result is that the signal strength is relatively similar, but that was not displayed by the figures produced. This observation is addressed in more detail in Chapter V.

Figure 13 is the G/T graph resulting from the Titan measurements shown in Figure 12.

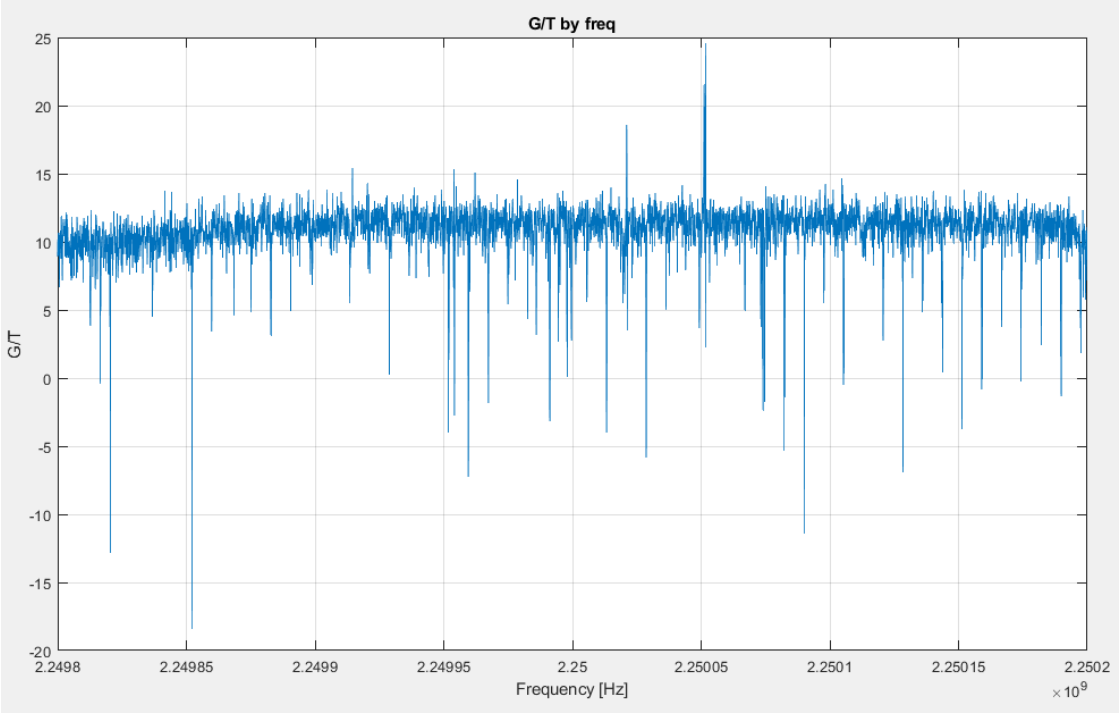

Figure 13. Titan G/T from 2.2498 to 2.2502 GHz (400 kHz span)

As expected, when collecting 4000 samples (about four times more than the FieldFox) over a much smaller frequency range, 400 kHz (250 times smaller than the FieldFox), the results demonstrate increased volatility. Observing the dramatic differences

in the two measurements (Figures 11 and 13) led us to take a new set of measurements with the FieldFox over the same 400 kHz frequency range. This decision was made in order to gain insight into this difference, as well as to provide a more consistent comparison between the two systems. Figure 14 is a sun and cold sky collection from the FieldFox over the same frequency range as the Titan's collection (2249.8 to 2250.2 MHz).

Figure 14. FieldFox Sun vs. Cold Sky Input Power from 2.2498 to 2.2502 GHz (400 kHz span)

When comparing both FieldFox collections, the 100 MHz and 400 kHz frequency ranges (Figure 10 and Figure 14), the major difference represented is the perspectives they offer. Figure 10 distinctly shows the natural waveforms seen in RF signals, making it easy to see any interference or other major degradations in the spectrum. Figure 14 demonstrates that you can still derive a reliable G/T value with this method. Other meaningful observations can't be made because the focus is too narrow when collecting over a 400 kHz range. Figure 15 (the FieldFox G/T graph of the 400 kHz range) examines the G/T

graph produced from the RF collection in Figure 14. Figure 15 is compared with the result from the Titan G/T graph, Figure 13.

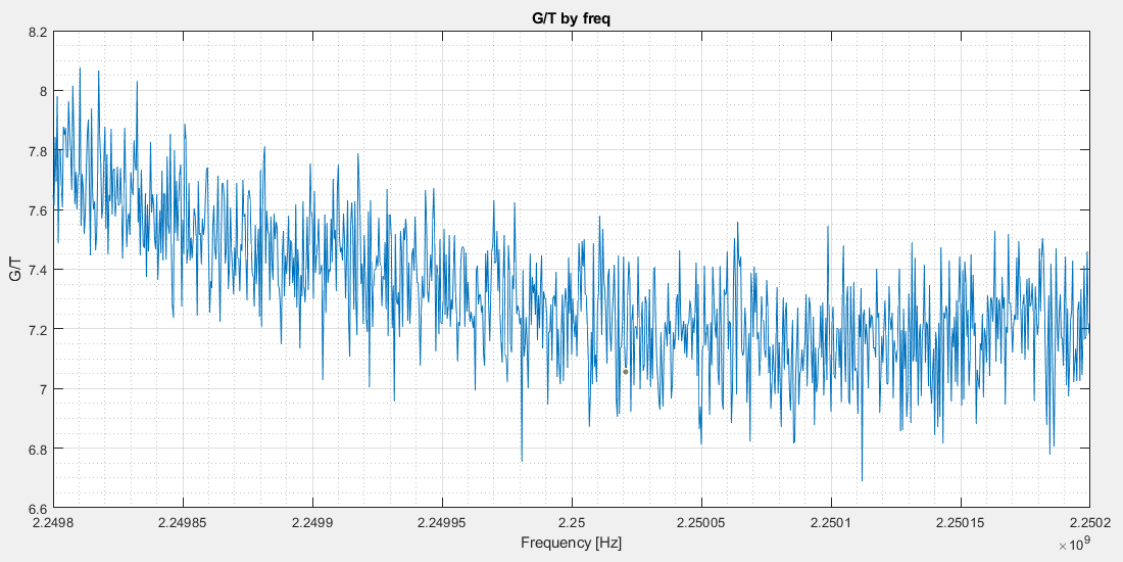

Figure 15. FieldFox G/T from 2.2498 to 2.2502 GHz (400 kHz span)

When comparing the FieldFox G/T (Figure 15) to the Titan G/T (Figure 13), it is obvious that the FieldFox demonstrates results that are more visually appealing. The resultant graph is expected because of the smaller sample size being displayed over the same frequency range. As observed, neither the FieldFox or Titan can provide observations such as interferference, over the entire 2.2 to 2.3 GHz range, with the small 400 kHz collection. However, both have sufficient fidelity to provide a health assessment that reliably conveys if the ground station is functioning or not.

The following portion of this chapter presents the results from the final test conducted for this thesis. In this test, we collected sun and cold sky RF remotely at NPS from three ground stations in the MC3 network. We collected this data nearly simultaneously to produce G/T graphs utilizing Titan. The two other ground stations involved in the test were AFIT and SDL. Figures 16 and 17 are the sun vs. cold sky input power and G/T graphs from AFIT.

Figures 16 and 17 demonstrate that the AFIT ground station is functioning normally. The results conveyed a reliable RF chain, and the ground station should expect normal operation. If the ground station was experiencing issues communicating with a satellite, the G/T graph produced would rule out any issues with the RF chain or antenna, and prompt the troubleshooting efforts to continue elsewhere.

Figures 18 and 19 are the sun vs. cold sky input power and G/T graphs from NPS.

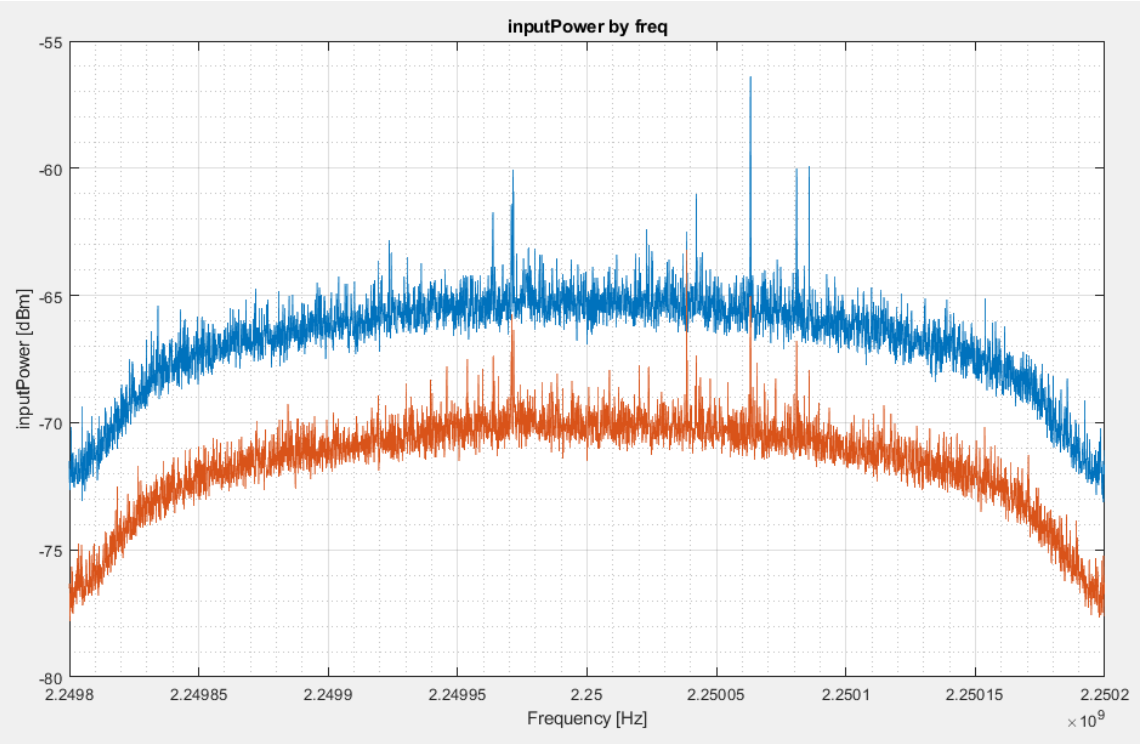

Figure 16. AFIT Titan Sun vs. Cold Sky Input Power from 2.2498 to 2.2502 GHz (400 kHz span)

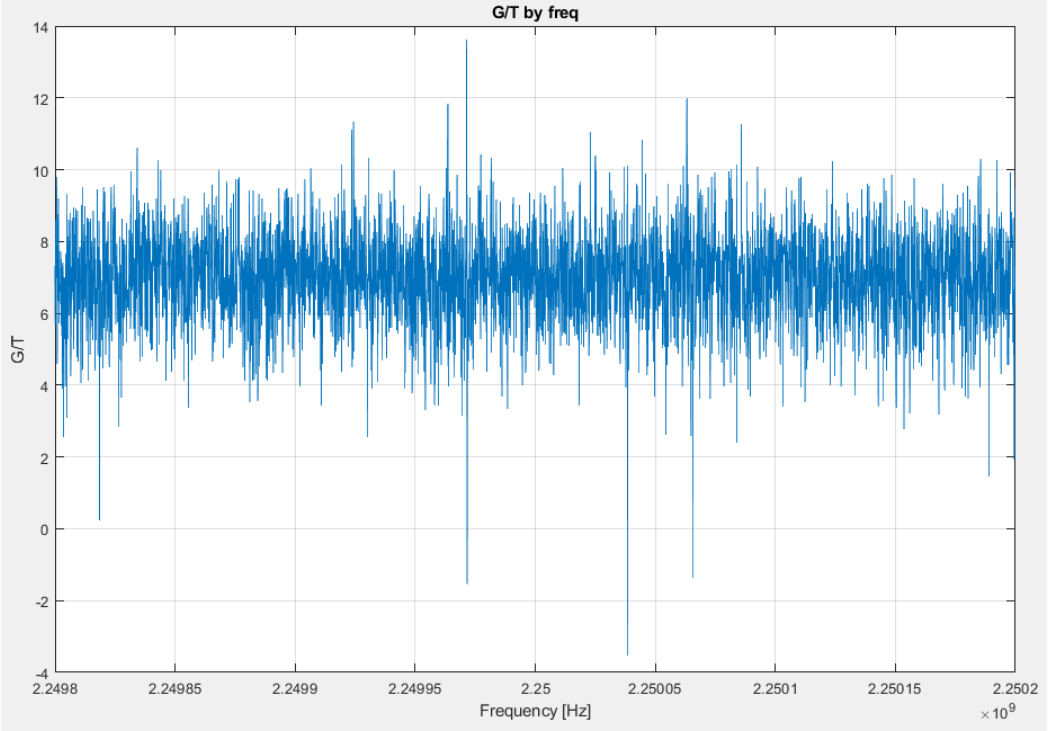

Figure 17. AFIT Titan G/T from 2.2498 to 2.2502 GHz (400 kHz Span)

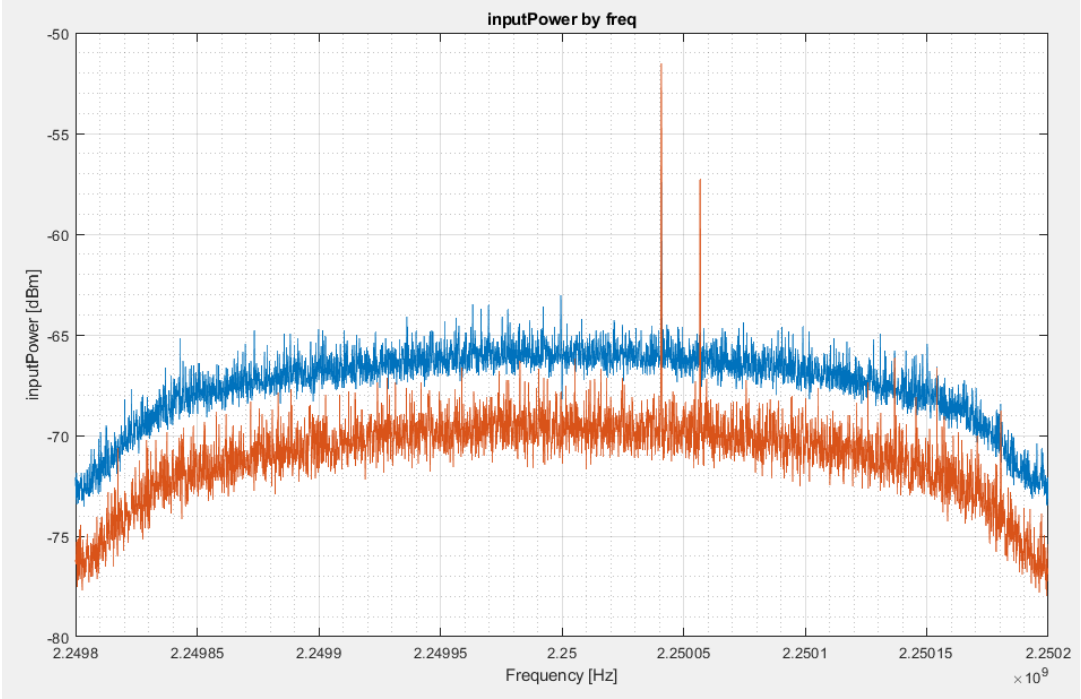

Figure 18. NPS Titan Sun vs. Cold Sky Input Power from 2.2498 to 2.2502 GHz (400 kHz span)

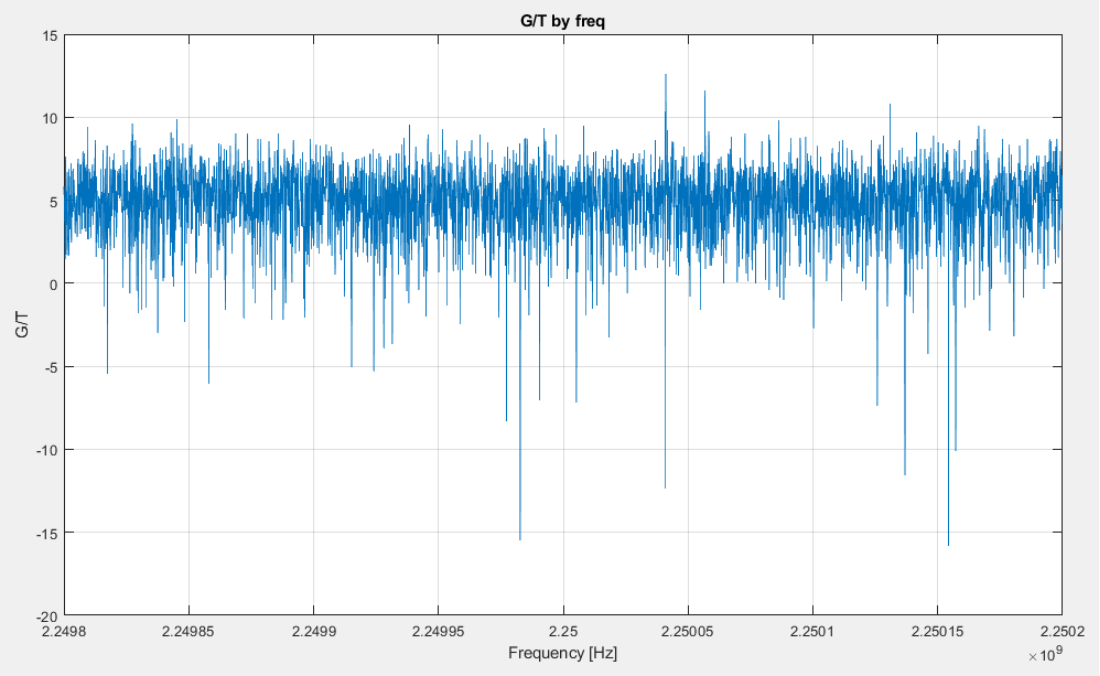

Figure 19. NPS Titan G/T from 2.2498 to 2.2502 GHz (400 kHz Span)

Similarly positive results were achieved with the NPS ground station G/T. The cold sky measurements are very similar when comparing the NPS input power (Figure 18) to AFIT (Figure 16), but the measured RF signal from the sun is stronger at the AFIT ground station. This is easier to notice when comparing the white space between the cold sky and sun measurements in Figure 18 to Figure 16. The larger *y*-value that was calculated at the AFIT ground station due to the greater P_{delta} collected, shown in Figure 16, indicates a higher expected G/T. Those results were confirmed and are demonstrated in Figures 17 and 19. The average G/T for AFIT is 7 compared to 5 for NPS.

Figures 20 and 21 are the sun vs. cold sky input power and G/T graphs from SDL.

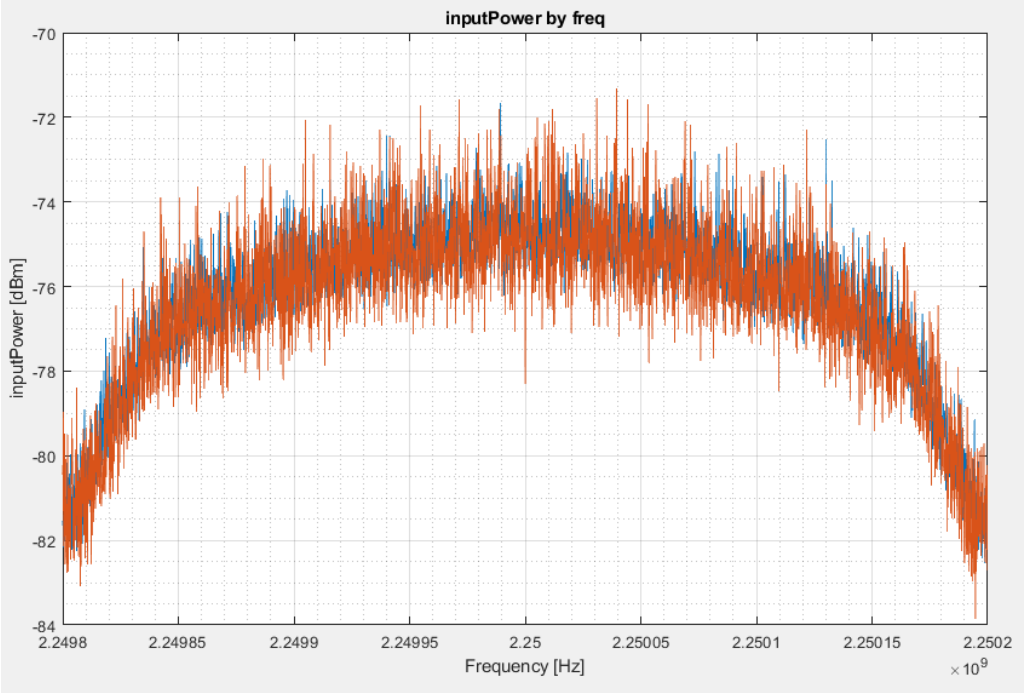

Figure 20. SDL Titan Sun vs. Cold Sky Input Power from 2.2498 to 2.2502 GHz (400 kHz span)

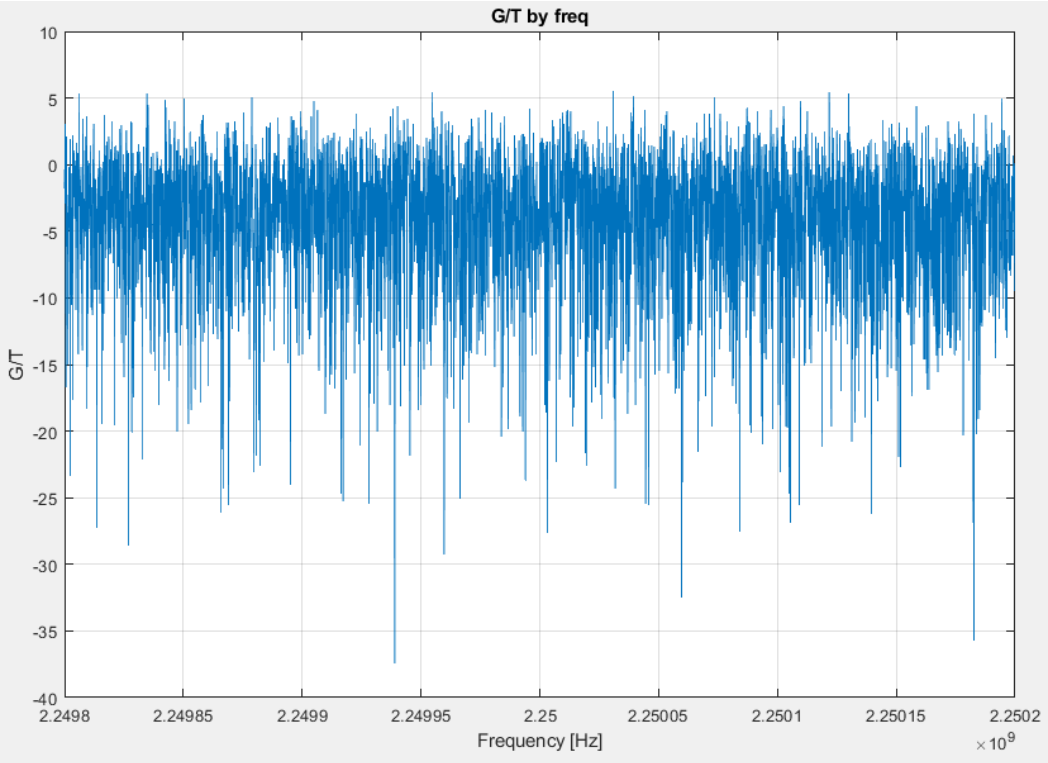

Figure 21. SDL Titan G/T from 2.2498 to 2.2502 GHz (400 kHz Span)

Figures 20 and 21 produced from the collection at the SDL ground station warrant further investigation. Based on Figure 21, SDL would have trouble communicating with any satellite at those frequencies because most of the G/T values are below zero. The poor G/T values were expected when Figure 20 was inspected. There was little to no separation between the sun and cold sky measurements, which produced a P_{delta} value of zero for most of the frequencies. A smaller P_{delta} value resulted in a smaller y-value, which severely impacted the G/T as displayed in Figure 21.

This was a very useful result because operators had reported a degraded downlink performance with their satellite at the time this measurement was taken. When we ran the G/T measurements, the weak performance was confirmed. Figures 20 and 21 were provided to the SDL engineers to aid with their investigation into the cause of the poor signal. While the cause was not determined prior to the completion of this thesis, we believe the issue to be RF-chain related specifically because of this measurement. The capability to produce a G/T graph, similar to Figure 21, to assess the health of an MC3 ground station further highlighted the advantage that this research can provide.

C. OVERALL STATUS

Based on the supporting data, our position is that utilizing the Titan to collect and process RF signals is a viable solution for calculating the system G/T. The resulting G/T that the Titan is able to produce has enough fidelity to provide a pass or fail status of the ground station's ability to communicate with satellites. Furthermore, it can be used as a baseline for troubleshooting potential issues. However, more work needs to be done prior to fully implementing this process into the NPS ground station, or for utilization throughout the MC3 network, which is discussed in Chapter V.

V. CONCLUSIONS

While the conclusions reached in this thesis are a positive step toward implementing a fully automatic health assessment for the NPS ground station, more work remains. Some of the topics that we recommend investigating further are expanding the spectrum collected, scientifically verifying the RF received, further automating the process, and utilizing alternate sources of RF to include using the moon.

A. EXPAND SPECTRUM COLLECTED

Expanding the spectrum collected should prove to be the most beneficial improvement, because it would enhance the value of the G/T automation process, allowing for maximum potential to be gained from any future improvements. Expanding the frequency range collected with confidence from 400 kHz is imperative to provide a better perspective of what is going on in the RF chain at the ground station. When possible, we recommend expanding the collection of RF to 100 MHz, similar to what is done with the FieldFox. However, if that proves too difficult with the technology available, another approach could be to collect multiple 400 kHz samples within the 2200 MHz to 2300 MHz range. This would be an alternate solution to expanding the frequency range to provide a similar perspective. Expanding the spectrum collected is the most important issue to address, regardless of the method used, to gain a broader perspective of the RF chain.

B. VERIFICATION OF RESULTS

An observation regarding the differences in RF signal strength collected by the FieldFox and Titan noted in Chapter IV can be addressed scientifically with the following recommended method. Using a signal generator connected to the splitter, provide a signal to both the Titan and FieldFox, then record and compare the results. It is recommended to collect and record the results with a variety of signal strengths—at least four—in order to have a large enough sample size to provide confidence in the results. The results should clarify if there are differences between the signal generated and signal received by both the Titan or FieldFox. The variation should explain the differences noticed in the graphs produced in Chapter IV. Once the differences are understood, a decision can be made as to

whether or not the variance in signal strength needs to be accounted for and managed within the software, or if the results are acceptable as produced.

C. AUTOMATION

Once the G/T process is developed to provide the frequency range for maximum result, the goal should be to focus on further automating the process. Some of the processes of automation to be addressed in future research should include programming the sun and cold sky RF data collected to be sent to a specified location and processed. Another area on which to focus is to develop a uniform naming system for the data to make this process more efficient as well. Once the data is processed and appropriately named, the final step for the automation process should be to send the data to a specified database. Once the final processed data is stored in the database, it can be recalled for analysis, whether on site or remotely. The benefit to having this data readily available is early identification of problem areas, troubleshooting, and ensuring the proper deployment of personnel when necessary. There will likely always be additional benefits to automation within the system, and additional areas that will need to be addressed. However, this list should represent a sufficient initial focus for items to investigate toward the goal of continued automation.

D. ALTERNATE RF SOURCES

A longer term goal is to expand the capability of the G/T calculation to include using other sources of RF. Once the data gathering and automation process is perfected for using the sun as the RF source, the next source of RF can be pursued. Using the moon as an alternate RF source is a natural progression for this capability, because as the MC3 network expands and services more users, the available free time for the ground stations to perform a G/T calculation will naturally be decreased. The limited time will require more RF source options be made available in order to continue taking the G/T calculation daily, or as may be required. The ability to use the moon as the RF source will allow ground stations the opportunity to take the measurements during the night. This capability will vastly expand the amount of time available to conduct the G/T calculation. However, the first step is perfecting the G/T calculation with the sun, especially considering the unique and challenging factors that will need to be addressed to use the moon as an RF source,

which was discussed in Chapter II. However, as the network grows and experiences ever increasing demand for its services, expanding the health assessments capabilities is the next logical step.

THIS PAGE INTENTIONALLY LEFT BLANK

LIST OF REFERENCES

[1] CDC, "COVID-19 and your health," *Centers for Disease Control and Prevention*, Feb. 11, 2020. Accessed May 04, 2021 [Online]. Available: https://www.cdc.gov/coronavirus/2019-ncov/travelers/map-and-travel-notices.html

[2] H. D. Griffiths and M. Libert, "Assessment of a technique for measurement of antenna G/T using solar noise," in *IEE Colloquium on Novel Antenna Measurement Techniques*, Jan. 1994, p. 6/1–6/6.

[3] C. Capela, "Protocol of communications for VORSAT satellite," M.S. thesis, Dept. of Elec. Eng., University of Porto, Porto, Portugal, 2012.

[4] B. Beicher, "Automation of antenna gain-to-noise temperature (G/T) measurements for a satellite communications system," M.S. thesis, Dept. of Space Sys., Bundeswehr University Munich, Munich, Germany, 2020.

[5] R. C. Griffith, "Mobile Cubesat Command and Control (MC3)," M.S. thesis, Dept. of Space Sys. Ops., Naval Postgraduate School, Monterey, California, USA, 2011.

[6] G. Minelli *et al.*, "The Mobile Cubesat Command and Control (MC3) ground station network," Naval Postgraduate School, USA, 2020 [Online]. Available: https://www.nasa.gov/sites/default/files/atoms/files/2020-05-20_mobile_cubesat_command_and_control_mc3_-_nasa_smallsat_virtual_institute_webinar.pdf

[7] "Link budget calculations for a satellite link with an electronically steerable antenna terminal." Kymeta, 2019 [Online]. Available: https://www.kymetacorp.com/wp-content/uploads/2020/09/Link-Budget-Calculations-2.pdf

[8] D. F. Wait, W. C. Daywitt, M. Kanda, and C. K. S. Miller, "A study of the measurement of G/T using Cassiopeia A," National Bureau of Standards, Fort Huachuca, AZ, Rep. 74-382, 1974 [Online]. Available: https://www.govinfo.gov/content/pkg/GOVPUB-C13-c5a1c4ce327b0c2d51604083c62a1d54/pdf/GOVPUB-C13-c5a1c4ce327b0c2d51604083c62a1d54.pdf

[9] M. Morgan, "Determination of earth station antenna G/T using the sun or the moon as an RF source," Orbital Systems Ltd., Irving, TX, USA, SSC18-X–05, 2018 [Online]. Available: https://digitalcommons.usu.edu/cgi/viewcontent.cgi?article=4128&context=smallsat

[10] K. F. Tapping, "The 10.7 cm solar radio flux (F10.7)," *Space Weather*, vol. 11, no. 7, pp. 394–406, 2013, doi: https://doi.org/10.1002/swe.20064

[11] D. Sˇekuljica, “Using the Moon as a calibrated noise source to measure the G/T figure-of-merit of an X-band satellite receiving station with a large antenna 200...400 wavelengths in diameter,” M.S. thesis, Univerza v Ljubljani, Ljubljana, Slovenia, 2017.

[12] M. H. Francis, “X-band atmospheric attenuation for an earth terminal measurement system,” National Institute of Standards and Technology, Gaithersburg, MD, USA, NIST IR 89–3918, 1989. doi: 10.6028/NIST.IR.89-3918

[13] T. J. Daim, M. Ismail, H. Salim, M. K. H. Ismail, and H. Mustapha, “A review of S-band antenna system G/T measurement technique,” in *2015 10th Asian Control Conference (ASCC)*, May 2015, pp. 1–6, doi: 10.1109/ASCC.2015.7244490

[14] K. G. Johannsen and L. Titus, “Determination of KU-band earth station antenna G/T using the moon as RF source,” *IEEE Transactions on Instrumentation and Measurement*, vol. IM–35, no. 3, pp. 344–348, Sep. 1986, doi: 10.1109/ TIM.1986.6499222

[15] G. Maral, M. Bousquet, and Z. Sun, *Satellite Communications Systems: Systems, Techniques and Technology*, 5th ed. Chichester, West Sussex, UK: John Wiley, 2009.

INITIAL DISTRIBUTION LIST

1. Defense Technical Information Center
   Ft. Belvoir, Virginia

2. Dudley Knox Library
   Naval Postgraduate School
   Monterey, California